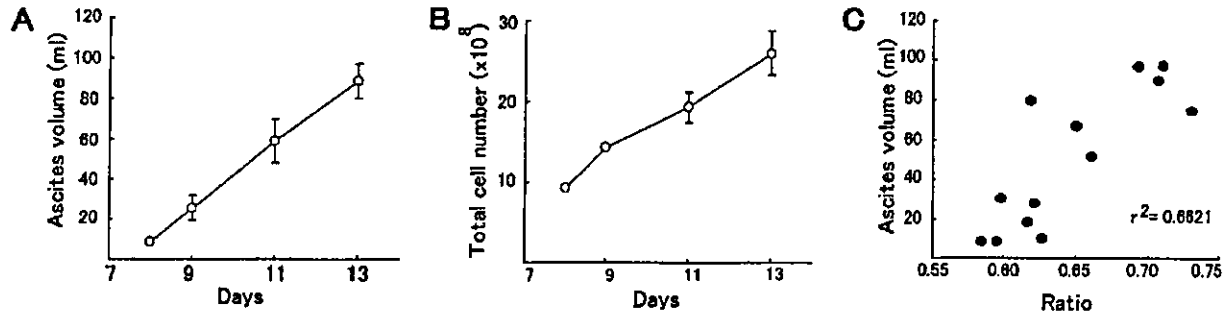

Figure 2. Characterization of the MM1 ascites model. (A and B), Kinetics of ascites accumulation and cell proliferation. The animals were sacrificed at various time points after intraperitoneal inoculation of MM1 cells. The ascites volume (A) and the total cell number (B) were determined as described. (C), Regression plot of the abdominal ratio versus ascites volume. Measurement of body size was performed immediately before sacrifice, and the ascites volume was then measured. Each dot represents an individual animal.

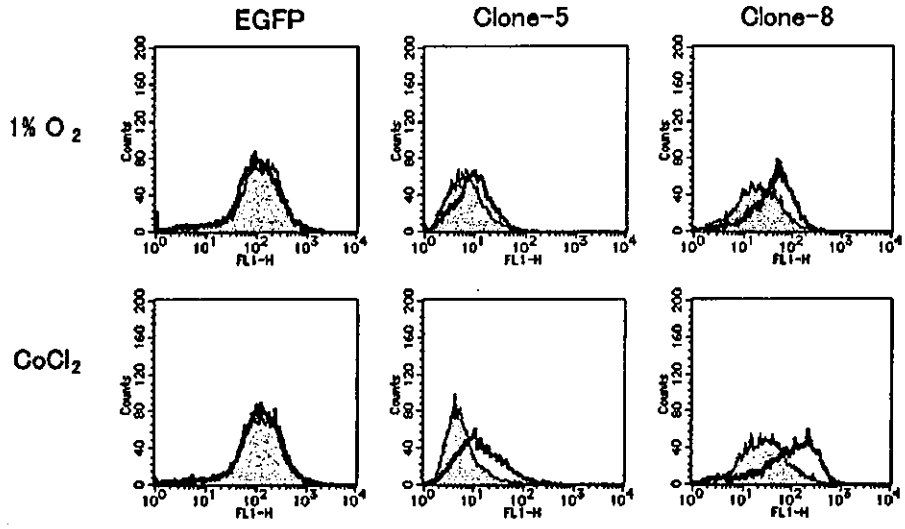

Figure 3. Conserved protein degradation machinery under normoxia via the ODD domain in MM1 cells *in vitro*. EGFP fluorescence from two different MM1 clones stably transfected with the pMX-NLS-ODD-EGFP vector was measured by flow cytometry. Three different clones were subjected to this experiment. EGFP represents a clone from pMXiresEGFP transfected MM1 cells, and clone-5, 8 are the clones from pMX-NLS-ODD-EGFP tranfected cells. Top panels are from cells cultured under normoxic (gray area) or 1% O_2 conditions (black line). The bottom panels are from cells cultured under normoxic conditions with (black line) or without (gray area) cobalt chloride. The experiments were repeated three times and the data shown are from a representative experiment.

ten (60%) treated animals showed a complete cure of ascites and lived as long as 200 days until being sacrificed for inspection of the abdominal cavity. No ascites or invasive cancer foci were observed in any of these animals. Three out of ten treated animals showed delayed ascites regression, and died after about 30 days.

The kinetics of the TOP3 effects was examined in detail (Fig. 5B) using the body measurement method described above. The pattern of ascites fluid accumulation in TOP3-treated animals was almost the same as that in untreated animals until day 14. However, all untreated rats died within 17 days while TOP3-treated animals survived for much longer. The ascites fluid gradually decreased in the TOP3-treated animals and returned to a normal level after 30 days.

Since the ascites volume increased to an equal extent until day 14, irrespective of the treatment, we examined the cell components of the ascites cytologically. As shown in Fig. 6A, a remarkable change was observed in the cell population pattern; the number of tumor cells decreased while monocyte/macrophage numbers increased in the TOP3-treated ascites fluid. There was a small number of neutrophils, but the cell population showed no change after treatment, and almost no lymphocytes were detected. Flow cytometric analysis also showed that ascites cells consisted of two major populations (Fig. 6B). In the ascites taken from untreated animals on day 13, most of the cells were tumor cells. In contrast, TOP3-treated ascites showed quite a different pattern, with less tumor cells and increased numbers of smaller cells. To confirm that these smaller cells were monocytes/macrophages, we analyzed the ascites cells with the monoclonal antibody CD11b, which recognizes monocytes and macrophages, as well as neutrophils (25). The gated smaller cell population that appeared after TOP3 treatment was indeed shown to be CD11b-positive (Fig. 6C). Taken together, these results suggest that TOP3 treatment decreased the number of tumor cells and increased monocyte and macrophage levels in ascites.

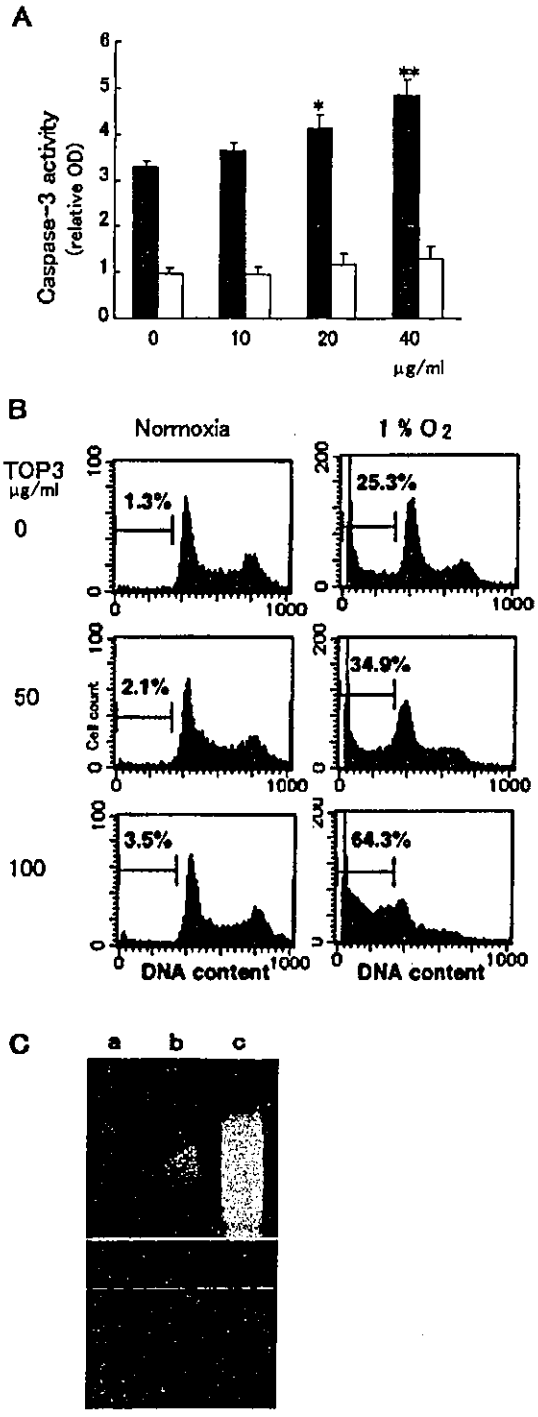

Figure 4. *In vitro* effects of TOP3 on MM1 cells. (A), Increase of caspase-3 activity by TOP3 under hypoxic conditions. MM1 cells were cultured under normoxic (open bars) or hypoxic (filled bars) conditions for 15 h. TOP3 was then added to achieve the indicated concentration. Relative caspase-3 activity with various TOP3 concentrations is presented as relative OD (mean of three independent experiments ± SD; $^{**}p<0.001$, $^{*}p<0.01$) compared with the caspase-3 activity of untreated hypoxic cells. (B), Increased cell death with TOP3 treatment under hypoxia. MM1 cells incubated under normoxic (left panel) or hypoxic (right panel) conditions with the indicated TOP3 concentration were subjected to DNA content analysis by flow cytometry. The percentage of apoptotic subG1 cells is shown. (C), DNA samples from the same cells as in (B) were subjected to electrophoresis for identification of DNA ladders. The data shown are from cells cultured under hypoxic conditions. TOP3 concentrations are 0 (a), 50 (b) and 100 (c) μg/ml, respectively.

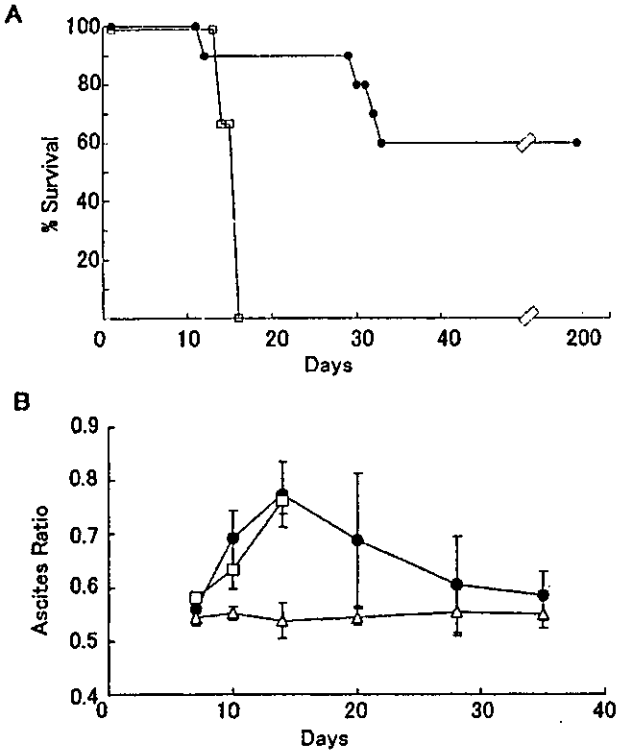

Figure 5. The anti-tumor effect of TOP3. (A), Prolonged survival due to TOP3 treatment of malignant ascites. TOP3 (●) (n=10) or buffer (□) (n=9) was injected intraperitoneally. The rats were monitored until day 200 when all surviving animals were sacrificed and subjected to autopsy to explore recurrent tumors. (B), Regression of ascites due to TOP3 treatment. The same animals as in (A) were subjected to body size measurements on day 7, 9, 13, 20, 27 and 34 to monitor ascites volume. Buffer-treated animals were measured only until day 13 because all of them died within 17 days. A group that was not challenged with tumor cells is shown as a control (Δ) (n=3). Values are the mean ± SD.

Discussion

A solid tumor is highly heterogeneous in terms of its micro-environment, including properties such as oxygen level, pH and concentration of nutrients (26). In comparison with this complexity, cultured hypoxic conditions might be too simplified to test hypoxia-targeting drugs appropriately. In contrast, malignant ascites are characterized by conditions that include hypoxia, low pH and low glucose concentration. It should also be noted that MM1 cells in ascites can survive and even divide in almost anoxic ascites fluid for several days, whilst cultured MM1 cells mostly die after 48 h under 1% oxygen conditions (data not shown). Moreover, in the ascites model, host response to the hypoxia-targeting therapy can be observed, such as the massive macrophage induction observed in this study.

Efficacy and drug delivery are the two major obstacles to be overcome in developing a tumor hypoxia therapy for solid tumors (27). In a hypoxic region, tumor cells are resistant to the death signal and some of them are not dividing, hence also making these cells resistant to conventional therapy. Drug delivery to the hypoxic region is difficult due to the interstitial pressure and/or the distance from blood vessels (28).

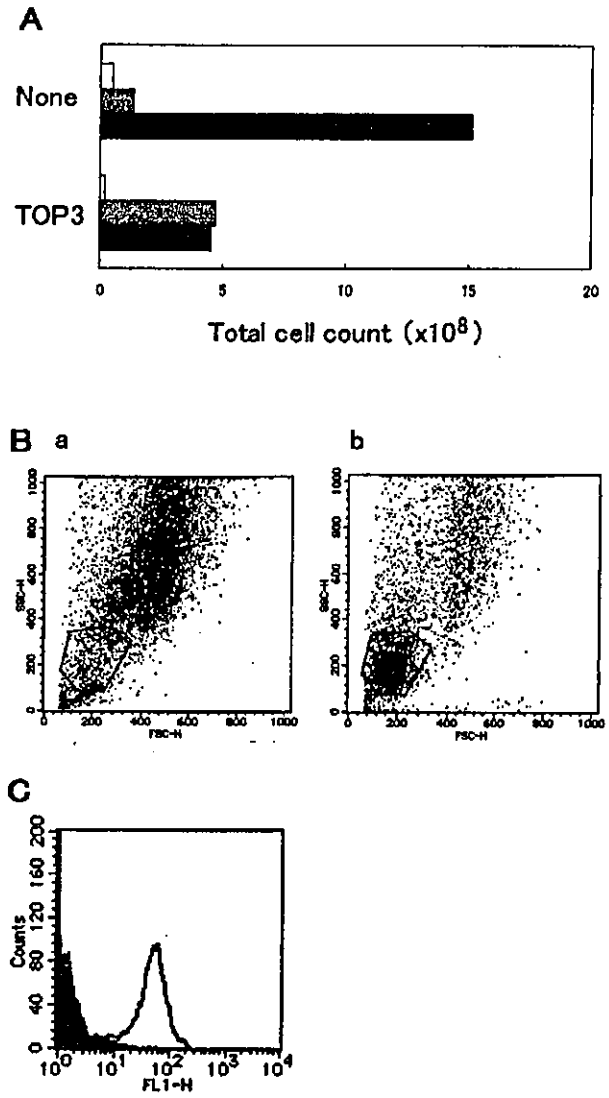

Figure 6. A decrease in the number of cancer cells and an increase of monocytes/macrophages in TOP3-treated ascites. (A), Ascites cells on day 13 were counted by morphology. Open bar, neutrophil; gray bar, monocyte/macrophage; and black bar, cancer cell. Three animals were examined and representative data are shown. (B), Ascites cells were examined by flow cytometry. The dot plot shows the ascites cells treated with the buffer (a) or TOP3 (b) on day 13. The percentage of the number of gated smaller-sized cells out of the total number of cells was 5.0% in untreated ascites (a) and 29.2% in TOP3-treated (b) ascites, respectively. (C), The population of smaller-sized cells induced by TOP3 treatment expressed the monocyte/macrophage surface antigen (CD11b). The ascites cells were stained with anti-CD11b antibody and analyzed by flow cytometry. The histogram shows a comparison of the stained (open peak) and unstained (closed peak) cells in the gated area from the TOP3-treated cells in (B, b).

TOP3 was designed to surmount these obstacles. However, evaluation of the efficacy of TOP3 *in vivo* by monitoring the size of a solid tumor might underestimate the effect of such hypoxia-targeting therapy, because the area of extreme hypoxia is just a small portion of the total tumor mass. Hence, to evaluate the efficacy of TOP3 *in vivo*, we utilized a malignant ascites model. The merits of this model are as follows. First, it provides a large number of homogeneous hypoxic cells that are adapted to hypoxia. Second, a drug can be easily delivered by intraperitoneal injection. Third, collection of ascites fluid is feasible and allows useful information about the mechanism of the drug effects to be obtained.

To monitor the ascites formation without intervention, previous studies have used body weight, circumference of the belly (29), or grading based only on the appearance of the animals (30). In our model, we also measured body weight, but found no significant correlation with ascites volume (data not shown). Body weight is influenced by multiple factors and any change should be defined as a net weight gain or loss during the experimental period. Animals are expected to gain weight due to ascites accumulation, as well as through natural growth, since they are in the stage of rapid growth, whereas they should lose weight due to severe cachexia caused by massive ascites formation (31). Based on the results presented here, we concluded that our body measurement method provides an easy and accurate estimation of ascites volume.

In malignant ascites of both patients and some animal models, a high level of VEGF has been reported (32,33). As VEGF potently induces vascular permeability, it might be one of the factors that promote ascites accumulation. Indeed, several reports have demonstrated that anti-VEGF treatments are effective against the formation of experimental ascites (30,34). Since hypoxia is one of the major inducers of VEGF expression (19), low oxygen tension in ascites fluid might be a causative factor in promoting VEGF expression and consequently ascites accumulation. In our model, ascites cells expressed higher levels of VEGF mRNA than cultured MM1 cells, and ascites fluid showed a high level of VEGF, as also found by ELISA in ascites models (data not shown). The decrease of VEGF in ascites after TOP3 treatment might directly impair ascites accumulation, since the effect of VEGF is quite sensitive to its level (35). To assess whether TOP3 is beneficial to patients with malignant ascites, the oxygen level of the malignant ascites will need to be analyzed.

We have demonstrated here that TOP3 has a dramatic effect both *in vitro* and *in vivo*. The mechanism through which TOP3 completely cured ascites may be rather complex, and two possibilities are apparent. One is a direct effect in which TOP3 directly induced apoptosis in ascites cancer cells, as was clearly observed in the experiments *in vitro*. The other is a more indirect effect of the host immune system, which may be triggered by massive tumor cell death following TOP3 treatment. The latter mechanism must at least be involved to some extent, since TOP3 treatment could not kill all the ascites cells directly. Indeed, the ascites cells recovered in the culture the day after the final TOP3 injection grew as fast as untreated MM1 cells (data not shown). As TOP3 injection induced a remarkable number of monocyte/macrophage in ascites, these host defense cells might produce such a secondary effect by presenting tumor antigen to the acquired immune system (36), secreting cytotoxic cytokines (37) or producing nitric oxide (38).

Our next concern, and one of paramount importance, is the use of TOP3 in combination with other cancer therapies, such as radiation therapy, chemotherapy and anti-angiogenesis therapy. As any hypoxia-targeting therapy, and especially that of TOP3, is specific to the hypoxic region, maximum efficacy should be expected when it is combined with other

therapies that are effective in the well-oxygenated region. We are now testing it in combination with radiotherapy, chemotherapy and anti-angiogenesis therapy.

Acknowledgements

This study was supported by a Grant-in-Aid for the Second-Term Comprehensive 10-Year Strategy for Cancer Control from the Ministry of Health, Labor and Welfare, Japan, and by the Ministry of Education, Science, Sports and Culture in Japan. We thank Toshio Kitamura for providing us with the pMX retroviral vectors, Naoko Harada for technical assistance, Hiroko Fukuda for cytological analysis, and Hiroyuki Nakamura for critical reading of the manuscript.

References

1. Graeber TG, Osmanian C, Jacks T, Housman DE, Koch CJ, Lowe SW and Giaccia AJ: Hypoxia-mediated selection of cells with diminished apoptotic potential in solid tumours. Nature 379: 88-91, 1996.
2. Magnusson KP, Satalino R, Qian W, Klein G and Wiman KG: Is conversion of solid into more anoxic ascites tumors associated with p53 inactivation? Oncogene 17: 2333-2337, 1998.
3. Blancher C and Harris AL: The molecular basis of the hypoxia response pathway: tumour hypoxia as a therapy target. Cancer Metastasis Rev 17: 187-194, 1998.
4. Pennacchietti S, Michieli P, Galluzzo M, Mazzone M, Giordano S and Comoglio PM: Hypoxia promotes invasive growth by transcriptional activation of the met proto-oncogene. Cancer Cell 3: 347-361, 2003.
5. Hockel M and Vaupel P: Tumor hypoxia: definitions and current clinical, biologic, and molecular aspects. J Natl Cancer Inst 93: 266-276, 2001.
6. Brown JM: Exploiting the hypoxic cancer cell: mechanisms and therapeutic strategies. Mol Med Today 6: 157-162, 2000.
7. Kung AL, Wang S, Klco JM, Kaelin WG and Livingston DM: Suppression of tumor growth through disruption of hypoxia-inducible transcription. Nat Med 6: 1335-1340, 2000.
8. Blouw B, Song H, Tihan T, Bosze J, Ferrara N, Gerber HP, Johnson RS and Bergers G: The hypoxic response of tumors is dependent on their microenvironment. Cancer Cell 4: 133-146, 2003.
9. Harada H, Hiraoka M and Kizaka-Kondoh S: Antitumor effect of TAT-oxygen-dependent degradation-caspase-3 fusion protein specifically stabilized and activated in hypoxic tumor cells. Cancer Res 62: 2013-2018, 2002.
10. Warburg O: On the origin of cancer cells. Science 123: 309-314, 1956.
11. Helmlinger G, Yuan F, Dellian M and Jain RK: Interstitial pH and pO_2 gradients in solid tumors *in vivo*: high-resolution measurements reveal a lack of correlation. Nat Med 3: 177-182, 1997.
12. Imamura F, Horai T, Mukai M, Shinkai K and Akedo H: Serum requirement for *in vitro* invasion by tumor cells. Jpn J Cancer Res 82: 493-496, 1991.
13. Nosaka T, Kawashima T, Misawa K, Ikuta K, Mui AL and Kitamura T: STAT5 as a molecular regulator of proliferation, differentiation and apoptosis in hematopoietic cells. EMBO J 18: 4754-4765, 1999.
14. Misawa K, Nosaka T, Morita S, Kaneko A, Nakahata T, Asano S and Kitamura T: A method to identify cDNAs based on localization of green fluorescent protein fusion products. Proc Natl Acad Sci USA 97: 3062-3066, 2000.
15. Morita S, Kojima T and Kitamura T: Plat-E: an efficient and stable system for transient packaging of retroviruses. Gene Ther 7: 1063-1066, 2000.
16. Livak KJ and Schmittgen TD: Analysis of relative gene expression data using real-time quantitative PCR and the 2[-Delta Delta C(T)] method. Methods 25: 402-408, 2001.
17. Imamura F, Shinkai K, Mukai M, Yoshioka K, Komagome R, Iwasaki T and Akedo H: rho-mediated protein tyrosine phosphorylation in lysophosphatidic-acid-induced tumor-cell invasion. Int J Cancer 65: 627-632, 1996.
18. Del Monte U: Changes in oxygen tension in Yoshida ascites hepatoma during growth. Proc Exp Biol Med 125: 853-856, 1967.
19. Shweiki D, Itin A, Soffer D and Keshet E: Vascular endothelial growth factor induced by hypoxia may mediate hypoxia-initiated angiogenesis. Nature 359: 843-845, 1992.
20. Shinohara Y, Hino M, Ishida T, Yamanaka Y and Terada H: Growth condition-dependent synchronized changes in transcript levels of type II hexokinase and type 1 glucose transporter in tumor cells. Biochim Biophys Acta 1499: 242-248, 2001.
21. Murphy BJ, Laderoute KR, Short SM and Sutherland RM: The identification of heme oxygenase as a major hypoxic stress protein in Chinese hamster ovary cells. Br J Cancer 64: 69-73, 1991.
22. Huang LE, Gu J, Schau M and Bunn HF: Regulation of hypoxia-inducible factor 1alpha is mediated by an O2-dependent degradation domain via the ubiquitin-proteasome pathway. Proc Natl Acad Sci USA 95: 7987-7992, 1998.
23. Vordermark D, Shibata T and Martin Brown J: Green fluorescent protein is a suitable reporter of tumor hypoxia despite an oxygen requirement for chromophore formation. Neoplasia 3: 527-534, 2001.
24. Salvesen GS and Dixit VM: Caspases: intracellular signaling by proteolysis. Cell 91: 443-446, 1997.
25. Robinson AP, White TM and Mason DW: Macrophage heterogeneity in the rat as delineated by two monoclonal antibodies MRC OX-41 and MRC OX-42, the latter recognizing complement receptor type 3. Immunology 57: 239-247, 1986.
26. Vaupel P, Kallinowski F and Okunieff P: Blood flow, oxygen and nutrient supply, and metabolic microenvironment of human tumors: a review. Cancer Res 49: 6449-6465, 1989.
27. Kizaka-Kondoh S, Inoue M, Harada H and Hiraoka M: Tumor hypoxia: a target for selective cancer therapy. Cancer Sci 94: 1021-1028, 2003.
28. Yu JL, Rak JW, Carmeliet P, Nagy A, Kerbel RS and Coomber BL: Heterogeneous vascular dependence of tumor cell populations. Am J Pathol 158: 1325-1334, 2001.
29. Hu L, Zaloudek C, Mills GB, Gray J and Jaffe RB: *In vivo* and *in vitro* ovarian carcinoma growth inhibition by a phosphatidylinositol 3-kinase inhibitor (LY294002). Clin Cancer Res 6: 880-886, 2000.
30. Mesiano S, Ferrara N and Jaffe RB: Role of vascular endothelial growth factor in ovarian cancer: inhibition of ascites formation by immunoneutralization. Am J Pathol 153: 1249-1256, 1998.
31. Tessitore L, Bonelli G and Baccino FM: Early development of protein metabolic perturbations in the liver and skeletal muscle of tumour-bearing rats. A model system for cancer cachexia. Biochem J 241: 153-159, 1987.
32. Kraft A, Weindel K, Ochs A, Marth C, Zmija J, Schumacher P, Unger C, Marme D and Gastl G: Vascular endothelial growth factor in the sera and effusions of patients with malignant and nonmalignant disease. Cancer 85: 178-187, 1999.
33. Luo JC, Yamaguchi S, Shinkai A, Shitara K and Shibuya M: Significant expression of vascular endothelial growth factor/vascular permeability factor in mouse ascites tumors. Cancer Res 58: 2652-2660, 1998.
34. Luo JC, Toyoda M and Shibuya M: Differential inhibition of fluid accumulation and tumor growth in two mouse ascites tumors by an antivascular endothelial growth factor/permeability factor neutralizing antibody. Cancer Res 58: 2594-2600, 1998.
35. Inoue M, Hager JH, Ferrara N, Gerber HP and Hanahan D: VEGF-A has a critical, non-redundant role in angiogenic switching and pancreatic beta cell carcinogenesis. Cancer Cell 1: 193-202, 2002.
36. Bellone M, Iezzi G, Rovere P, Galati G, Ronchetti A, Protti MP, Davoust J, Rugarli C and Manfredi AA: Processing of engulfed apoptotic bodies yields T cell epitopes. J Immunol 159: 5391-5399, 1997.
37. Maekawa H, Iwabuchi K, Nagaoka I, Watanabe H, Kamano T and Tsurumaru M: Activated peritoneal macrophages inhibit the proliferation of rat ascites hepatoma AH-130 cells via the production of tumor necrosis factor-alpha and nitric oxide. Inflamm Res 49: 541-547, 2000.
38. Nishikawa M, Sato EF, Kuroki T, Utsumi K and Inoue M: Macrophage-derived nitric oxide induces apoptosis of rat hepatoma cells *in vivo*. Hepatology 28: 1474-1480, 1998.

THE JOURNAL OF BIOLOGICAL CHEMISTRY
Vol. 279, No. 25, Issue of June 18, pp. 26176–26183, 2004
Printed in U.S.A.

Cyclic AMP Promotes cAMP-responsive Element-binding Protein-dependent Induction of Cellular Inhibitor of Apoptosis Protein-2 and Suppresses Apoptosis of Colon Cancer Cells through ERK1/2 and p38 MAPK*

Received for publication, December 5, 2003, and in revised form, March 18, 2004
Published, JBC Papers in Press, April 12, 2004, DOI 10.1074/jbc.M313346200

Hiroshi Nishihara‡, Michael Hwang‡, Shinae Kizaka-Kondoh§, Lars Eckmann¶, and Paul A. Insel‡¶‖

From the Departments of ‡Pharmacology and ¶Medicine, University of California, San Diego, La Jolla, California 92093-0636 and the §Department of Molecular Oncology, Kyoto University Graduate School of Medicine, Kyoto 606-8501, Japan

We recently reported that cAMP suppresses apoptosis in colon cancer cells and induces cellular inhibitor of apoptosis protein-2 (c-IAP2) via a cAMP-responsive element (CRE), suggesting a mechanism for chemoprevention of colon cancer by non-steroidal anti-inflammatory drugs. In this study, we used T84 human colon cancer cells to define the pathway by which increases in cAMP induce c-IAP2 expression. Treatment with several different cAMP agonists stimulated phosphorylation of CRE-binding protein (CREB) and activated expression of c-IAP2 in a CREB-dependent manner. Studies with pharmacological inhibitors revealed that cAMP-dependent phosphorylation of CREB required activation of ERK1/2 and p38 MAPK but was largely independent of protein kinase A. Immunoblots and transcriptional reporter assays using specific inhibitors, as well as expression of constitutively active forms of MEK1 and MKK3, showed that c-IAP2 induction by cAMP is regulated predominantly through ERK1/2 and p38 MAPK and suggested involvement of p90 ribosomal protein S6 kinase and mitogen and stress response kinase-1 as well. Consistent with those results, we found that cAMP-dependent suppression of apoptosis was blocked by treatment with inhibitors of ERK1/2 and p38 MAPK. We conclude that cAMP can induce c-IAP2 expression in colon cancer cells through CREB phosphorylation and CRE-dependent transcription in a manner that involves activation of ERK1/2 and p38 MAPK. These results emphasize that activation of kinases other than protein kinase A can mediate the actions of agents that increase cAMP, particularly in the regulation of CREB-dependent events.

Suppression of normal apoptotic pathways contributes to tumor progression and confers resistance to cytotoxic anticancer drugs and radiation (1). The second messenger cAMP has antiapoptotic actions (2–4), and its primary effector enzyme, PKA,[1] is a target for cancer therapy (5–7). Prostaglandin E_2 (PGE_2), which is formed from arachidonic acid by cyclooxygenases, binds to G_s-coupled receptors and increases intracellular cAMP concentration (8). Cyclooxygenase levels are high in human colon cancers (9), and cyclooxygenase inhibition prevents cell proliferation and promotes apoptosis (10, 11). Recently we reported that increases in cAMP levels promoted by PGE_2 or other agents that raise cAMP inhibit apoptosis in colon cancer cells through the induction of c-IAP2, therefore suggesting a novel mechanism of cancer chemoprevention by non-steroidal anti-inflammatory drugs (12).

Inhibitors of apoptosis proteins (IAPs) are characterized by a domain of about 70 amino acids, termed the baculoviral IAP repeat (BIR), based on the original discovery of these apoptosis suppressors in the baculoviral genome (13, 14). IAP family proteins have potentially important roles in the regulation of apoptosis and tumorigenesis (15, 16). The expression of survivin, one of the IAP family proteins, is significantly increased in several human cancers (17). Although eight human IAPs have been identified (18), c-IAP1/BIRC2 and c-IAP2/BIRC3 are the only IAPs that appear to be part of a signaling complex recruited to the cytoplasmic domain of the type 2 TNF receptor (19). In addition, c-IAP2 was also suggested to be a causative gene of mucosa-associated lymphoid tissue lymphoma and to have a role in carcinogenesis and tumor progression (20). The active forms of caspase-3 and -7 are directly inhibited by c-IAP2 (19), which can also prevent the proteolytic processing of procaspase-3, -6, and -7 by blocking the cytochrome *c*-induced activation of procaspase-9 (21).

Expression of c-IAP2 is regulated through multiple regulatory elements in its promoter region. A NF-κB binding site is essential for induction by TNFα in Jurkat T cells (22) and radiation in human embryonic kidney 293 cells (23). Dexamethasone induces c-IAP2 expression through a putative glucocorticoid response element in A549 human lung cancer cells (24), while a cAMP-responsive element (CRE) has an essential role in induction of c-IAP2 expression by cAMP in T84 colon cancer cells (12).

* This work was supported by grants from the National Institutes of Health, the Rebecca and John Moores University of California, San Diego (UCSD) Cancer Center, and the Sam and Rose Stein Institute for Research on Aging. The costs of publication of this article were defrayed in part by the payment of page charges. This article must therefore be hereby marked "*advertisement*" in accordance with 18 U.S.C. Section 1734 solely to indicate this fact.

‖ To whom correspondence should be addressed: Dept. of Pharmacology, University of California, San Diego, 9500 Gilman Dr., La Jolla, CA 92093-0636. Tel.: 858-534-2295; Fax: 858-822-1007; E-mail: pinsel@ucsd.edu.

[1] The abbreviations used are: PKA, protein kinase A; IAP, inhibitor of apoptosis proteins; c-IAP, cellular IAP; CRE, cAMP-responsive element; CREB, CRE-binding protein; ERK, extracellular signal-regulated kinase; MAPK, mitogen-activated protein kinase; RSK, ribosomal protein S6 kinase; MEK, mitogen-activated protein kinase/extracellular signal-regulated kinase kinase; MKK, MAPK kinase; MSK, mitogen and stress response kinase; PGE_2, prostaglandin E_2; BIR, baculoviral IAP repeat; TNF, tumor necrosis factor; mAb, monoclonal antibody; CTX, cholera toxin; 8-CPT-cAMP, 8-(4-chlorophenylthio)-cAMP; Fsk, forskolin; (R_p)-cAMPS, adenosine 3',5'-cyclic monophosphothioate, R_p isomer; 8-CPT-2'-*O*-Me-cAMP, 8-(4-chlorophenylthio)-2'-*O*-methyl-cAMP; WT, wild type; CHO, Chinese hamster ovary; ATF-2, activating transcription factor-2.

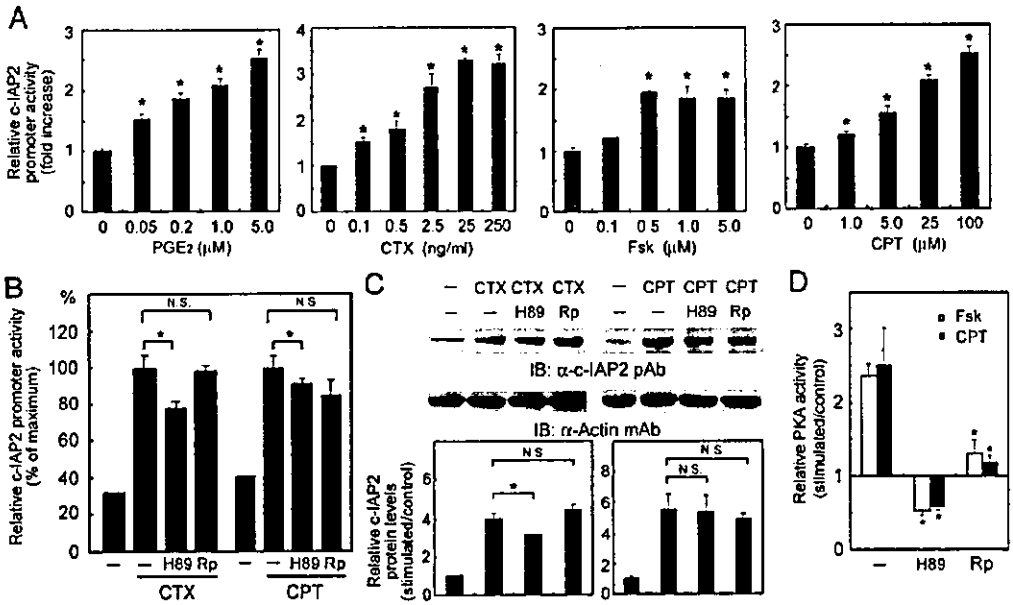

FIG. 1. **cAMP induces c-IAP2 expression primarily through PKA-independent pathways.** *A*, T84 cells, transfected with pGL3-c-IAP2-WT-Luc and pSV40-RL-Luc, were stimulated for 6 h with PGE_2, Fsk, or 8-CPT-cAMP (*CPT*) or for 12 h with CTX at the indicated concentrations. Cell extracts were assayed by a dual luciferase assay. Results represent relative increases compared with untreated controls and are mean ± S.E. ($n = 4$; *, $p < 0.05$ *versus* controls, respectively). *B*, T84 cells, transfected with pGL3-c-IAP2-WT-Luc and pSV40-RL-Luc, were treated with H89 (10 μM) or (R_p)-cAMPS (*Rp*, 100 μM) for 1 h and stimulated for 6 h with 8-CPT-cAMP (*CPT*, 100 μM) or 12 h with CTX (250 ng/ml). CTX and CPT both significantly increased c-IAP2 promoter activity in the absence or presence of inhibitors ($p < 0.05$). Results shown represent relative promoter activity compared with CTX- or CPT-treated cells without inhibitors as 100% and are mean ± S.E. ($n = 3$; *, $p < 0.05$; *N.S.*, not significant). *C*, T84 cells were treated for 1 h with H89 (10 μM) or (R_p)-cAMPS (*Rp*, 100 μM) and further stimulated for 6 h with 8-CPT-cAMP (*CPT*, 100 μM) or 12 h with CTX (250 ng/ml). Cells were lysed in SDS sample buffer, and proteins were analyzed by immunoblotting with the indicated antibodies. The *bottom graphs* show densitometric results of the respective blots normalized against actin levels and expressed relative to unstimulated controls and are mean ± S.E. ($n = 3$; *, $p < 0.05$; *N.S.*, not significant). CTX and CPT both significantly increased c-IAP2 protein expression in the absence or presence of inhibitors ($p < 0.05$). *D*, T84 cells, serum-starved for 12 h, were treated with H89 (10 μM) or (R_p)-cAMPS (*Rp*, 100 μM) for 1 h and stimulated with Fsk (1 μM) or 8-CPT-cAMP (*CPT*, 100 μM) for 3 min. Cell extracts were assayed for PKA activity using the PepTag assay. Results represent relative changes in PKA activity compared with untreated controls and are mean ± S.E. ($n = 3$; *, $p < 0.05$ *versus* Fsk- or CPT-treated cells without inhibitors, respectively). *IB*, immunoblot; *pAb*, polyclonal antibody.

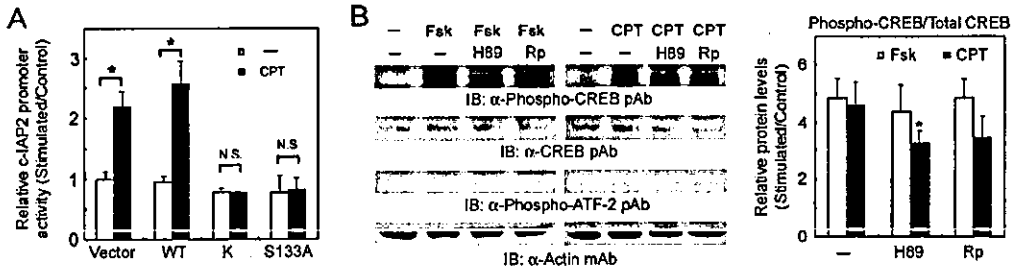

FIG. 2. **cAMP stimulates c-IAP2 promoter activity through phosphorylation of CREB.** *A*, T84 cells, transfected with pCMV-HA (*Vector*), pCMV-CREB WT (*WT*), pCMV-KCREB (*K*), or pCMV-CREB S133A (*S133A*); pGL3-c-IAP2-CREII-Luc; and pSV40-RL-Luc, were stimulated for 6 h with 8-CPT-cAMP (*CPT*, 100 μM). Cell extracts were assayed by a dual luciferase assay. Results represent relative increases compared with vector-transfected, untreated controls and are mean ± S.E. ($n = 3$; *, $p < 0.05$; *N.S.*, not significant, respectively). *B*, T84 cells were serum-starved for 12 h and incubated for 1 h with or without H89 (10 μM) and (R_p)-cAMPS (*Rp*, 100 μM) as indicated. After 30 min of further incubation with Fsk (1 μM) or 8-CPT-cAMP (*CPT*, 100 μM), cells were lysed in SDS sample buffer, and proteins were analyzed by immunoblotting with the indicated antibodies. The *right graph* shows densitometric results of the blots for phospho-CREB normalized to total CREB expression. Data are expressed relative to unstimulated cells without inhibitors and are mean ± S.E. ($n = 3$; *, $p < 0.05$ *versus* Fsk- or CPT-treated cells without inhibitors, respectively). *IB*, immunoblot; *pAb*, polyclonal antibody.

In this study, we analyzed the signal transduction pathways that mediate induction of c-IAP2 in response to increases in cAMP in T84 cells. We show that cAMP-promoted phosphorylation of CREB and transcriptional activation of c-IAP2 appear in large part to be mediated by activation of ERK1/2 and p38 MAPK, perhaps acting via p90RSK and MSK1.

EXPERIMENTAL PROCEDURES

Antibodies and Reagents—Anti-c-IAP2 polyclonal antibody and anti-actin monoclonal antibody (mAb) were from Chemicon International (Temecula, CA) and Santa Cruz Biotechnology (Santa Cruz, CA), respectively. Polyclonal antibodies against CREB, phospho-CREB, phospho-MSK1, phospho-p90RSK, p44/42 MAPK, phospho-p44/42 MAPK, p38 MAPK, and phospho-p38 MAPK and the MEK1/2 inhibitors PD98059 and U0126 were obtained from Cell Signaling Technology Inc. (San Diego, CA). mAb against Rap1 was from BD Bioscience Pharmingen. Cholera toxin (CTX), 8-CPT-cAMP, forskolin (Fsk), human recombinant TNFα, phorbol 12-myristate 13-acetate, H89, (R_p)-cAMPS, SB203580, and SB202190 were from Calbiochem. PGE_2 was from Sigma. 8-CPT-2′-*O*-Me-cAMP was purchased from BIOLOG Life Science Institute (Bremen, Germany).

Plasmids—pCMV-HA (vector control), pCMV-CREB (wild-type CREB), pCMV-KCREB (dominant negative form), and pCMV-CREB

S133A (dominant negative form) were purchased from Clontech. pUSE-MEK1 (S218D/S222D) (dominant active form) was purchased from Upstate Biotechnology (Lake Placid, NY). pBabeHygro-MKK3A (S189E/T193E) (dominant active form) was a gift from Dr. Peiqing Sun (25). pGL3-c-IAP2-WT-Luc (−1931 to +27) and pGL3-c-IAP2-CREII-Luc (−87 to +27) were described previously (12).

Cell Culture—T84 human colon epithelial cells were cultured in 50% Dulbecco's modified Eagle's medium, 50% Ham's F-12 medium supplemented with 5% newborn calf serum and 2 mM L-glutamine. Chinese hamster ovary (CHO) cells were cultured in Ham's F-12 medium supplemented with 10% fetal bovine serum and 2 mM L-glutamine.

Immunoblot Analysis—For detection of phospho-ERK1/2 and phospho-p38 MAPK, cells were lysed in 1% Triton X-100, 10 mM Tris-HCl (pH 7.4), 5 mM EDTA, 150 mM NaCl, 0.5 mM Na_3VO_4, 10 mM NaF, 1 μg/ml aprotinin, and 1 mM phenylmethylsulfonyl fluoride. For detection of other proteins, cells were lysed in 1× SDS sample buffer and sonicated twice for 15 s. Proteins were separated by SDS-PAGE and analyzed by immunoblotting with the indicated antibodies. Specific binding was visualized by Super Signal West Dura extended duration substrate (Pierce) and quantified by using an EpiChemi II darkroom image analyzer (Ultraviolet Products).

Dual Luciferase Assay—T84 cells in 24-well plates were transfected using the FuGENE 6 transfection reagent (Roche Applied Science) with pGL3-c-IAP2 (−1931 to +27) or pGL3-c-IAP2-CREII-Luc (−87 to +27), pRL-SV40-Luc (Promega, Madison, WI) carrying *Renilla* luciferase under the control of a constitutively active SV40 promoter as a transfection control, and CREB, MEK1, or MKK3 expression vectors as indicated in the figure legends. The dual luciferase assay was conducted with a dual luciferase reporter assay system (Promega).

PKA Activity Assay—Kinase activity of PKA was assayed with the PepTag® assay (Promega). Briefly T84 cells serum-starved for 6 h were treated for 1 h with H89 (10 μM) or (R_p)-cAMPS (100 μM) and stimulated with Fsk or 8-CPT-cAMP for 3 min. Cells were washed with phospate-buffered saline twice and lysed in lysis buffer (1% Nonidet P-40, 150 mM Tris-HCl, pH 7.5, 50 mM NaCl, 10 mM NaF, 1 mM phenylmethylsulfonyl fluoride). Lysates containing 8 μg of total protein were incubated with 2 μg of PepTag A1 peptide in reaction buffer for 8 min. Phosphorylated peptide was separated by 0.8% agarose gel electrophoresis and quantified by using an EpiChemi II darkroom image analyzer.

ERK1/2 and p38 MAPK Kinase Assay—Kinase activities of ERK1/2 and p38 MAPK were assayed with a p44/42 MAPK assay kit (non-radioactive) and p38 MAPK assay kit (non-radioactive) (Cell Signaling Technology Inc.), respectively. Briefly T84 cells were preincubated with inhibitors for 1 h followed by incubation with 8-CPT-cAMP for 30 min. Cells were lysed in lysis buffer and centrifuged at 20,000 × *g* for 10 min. The supernatants were incubated with immobilized anti-phospho-p44/42 MAPK or anti-phospho-p38 MAPK mAb for 4–12 h. Precipitated kinases were incubated with Elk or activating transcription factor-2 (ATF-2) fusion protein for 30 min in kinase reaction buffer containing 200 μM ATP, and phosphorylation of fusion proteins was detected by immunoblotting with phosphospecific antibodies.

Rap1 Pull-down Assay—Cells were serum-starved overnight and incubated with inhibitors for 1 h followed by further stimulation as indicated in the figure legends. Cell were lysed in lysis buffer (1% Nonidet P-40, 25 mM HEPES (pH 7.4), 150 mM NaCl, 10% glycerol, 1 mM EDTA, 10 mM $MgCl_2$, 0.5 mM Na_3VO_4, 10 mM NaF, 1 μg/ml aprotinin, and 1 mM phenylmethylsulfonyl fluoride) and centrifuged at 20,000 × *g* for 1 min. The supernatants were incubated with 15 μg of an agarose conjugate of Ral GDS-Rap binding domain (Upstate Biotechnology) for 45 min, and the beads were washed with lysis buffer three times. The precipitates were separated by SDS-PAGE and analyzed by immunoblotting with anti-Rap1 mAb.

Analysis of Apoptosis—T84 cells were incubated with inhibitors for 1 h followed by further incubation with CTX or 8-CPT-cAMP for 1 h. Cells were stimulated with staurosporine for 12 h and lysed in lysis buffer. After centrifugation of cells at 250 × *g* for 5 min, supernatants were isolated and assayed with the Cell Death Detection enzyme-linked immunosorbent assay PLUS kit (Roche Applied Science).

Caspase-3 Assay—Caspase-3 activity was assayed with a colorimetric assay kit (R&D Systems, Minneapolis, MN).

Data Presentation and Analysis—Results are shown as mean ± S.E. of at least three experiments as indicated in the figure legends. Comparisons between experimental groups were by paired or unpaired *t* test as appropriate with $p < 0.05$ considered significant.

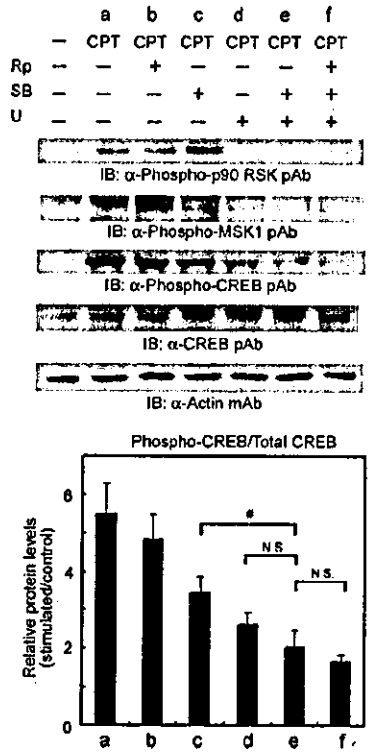

FIG. 3. **CREB phosphorylation is mediated by ERK1/2 and p38 MAPK.** T84 cells were serum-starved for 12 h and incubated for 1 h with SB202190 (*SB*, 20 μM), U0126 (*U*, 10 μM), and (R_p)-cAMPS (*Rp*, 100 μM) alone or in combination as indicated. After 30 min of further incubation with 8-CPT-cAMP (*CPT*, 100 μM), cells were lysed in SDS sample buffer, and proteins were analyzed by immunoblotting with the indicated antibodies. The *lower graph* shows densitometric results of the blots for phospho-CREB normalized to total CREB expression. Data are expressed relative to unstimulated controls without inhibitors and are mean ± S.E. ($n = 3$; *, $p < 0.05$; *N.S.*, not significant). Inhibitors, with the exception of (R_p)-cAMPS alone (*lane b*), significantly decreased CREB phosphorylation (*lanes c–f*, $p < 0.05$). *IB*, immunoblot; *pAb*, polyclonal antibody.

RESULTS

cAMP Induces c-IAP2 Expression Predominantly through PKA-independent Pathways in T84 Colon Epithelial Cells—We have previously shown that increases in cellular cAMP levels can transcriptionally induce c-IAP2 expression in T84 cells (12). To characterize the underlying mechanisms, we investigated the effects of multiple agents that raise cellular cAMP concentrations to regulate the activity of a full-length transcriptional reporter of c-IAP2. PGE_2 binds to G_s-coupled EP2 and EP4 receptors on colon epithelial cells and increases intracellular cAMP concentration (26, 27). Fsk directly stimulates adenylyl cyclase activity and increases cAMP production. We also used CTX, which catalyzes the ADP-ribosylation of G_s leading to the activation of adenylyl cyclase, and the membrane-permeant cAMP analog 8-CPT-cAMP. Stimulation of T84 cells with all four agonists that raise intracellular cAMP increased c-IAP2 promoter activity in a concentration-dependent manner (Fig. 1*A*).

To begin to define the downstream signaling mechanism for the cAMP-promoted increase in c-IAP2 promoter activity, we first focused on the role of PKA, the major effector kinase that mediates the action of cAMP. Surprisingly two different pharmacological inhibitors of PKA, H89 (10 μM) and (R_p)-cAMPS (100 μM), showed only limited inhibition (<25%) of cAMP-dependent increases in c-IAP2 promoter activity (Fig. 1*B*) and

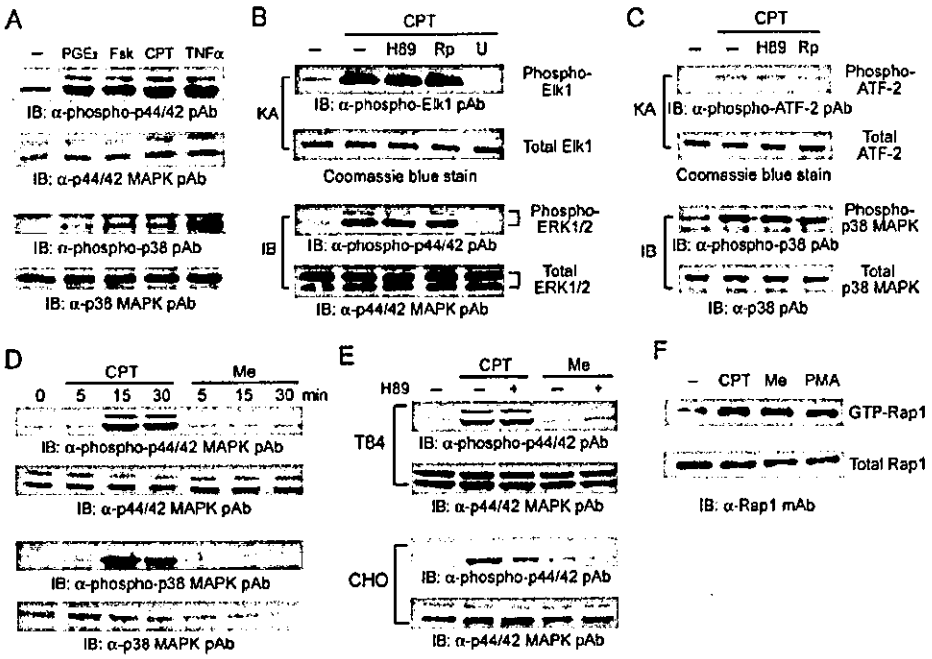

FIG. 4. **cAMP activates ERK1/2 and p38 MAPK in a PKA-independent manner.** *A*, T84 cells were serum-starved for 12 h and treated with PGE_2 (1 μM), Fsk (10 μM), 8-CPT-cAMP (*CPT*, 100 μM), or TNFα (100 ng/ml) for 30 min. Cells were lysed and analyzed by immunoblotting with the indicated antibodies. *B* and *C*, cells, serum-starved for 12 h, were treated with H89 (10 μM), (R_p)-cAMPS (*Rp*, 100 μM), or U0126 (*U*, 10 μM) for 1 h and incubated with 8-CPT-cAMP (*CPT*, 100 μM) for 30 min. Cell lysates were prepared and analyzed by non-radioactive kinase assay (*KA*). Immunoprecipitated phospho-ERK1/2 or phospho-p38 MAPK were incubated with Elk or ATF-2 fusion protein for 30 min at 30 °C in the presence of ATP (200 μM), and phosphorylated fusion proteins were analyzed by immunoblotting with the indicated antibodies (*KA*, *top panel*). The total amount of fusion protein present in each reaction was visualized by Coomassie Blue staining (*KA*, *second panel*). Total cell lysates were analyzed in parallel by immunoblotting (*IB*) with the indicated antibodies (*third* and *fourth panels*). *D* and *E*, T84 cells (*D*), serum-starved for 12 h, or CHO cells (*E*) were treated with H89 (10 μM) for 1 h and incubated with 8-CPT-cAMP (*CPT*, 100 μM) or 8-CPT-2′-*O*-Me-cAMP (*Me*, 100 μM) for the indicated times (*D*) or 15 min (*E*). Cells were lysed and analyzed by immunoblotting with indicated antibodies. *F*, T84 cells, serum-starved for 12 h, were incubated with 8-CPT-cAMP (*CPT*, 100 μM), 8-CPT-2′-*O*-Me-cAMP (*Me*, 100 μM), or phorbol 12-myristate 13-acetate (*PMA*, 1 μM) for 2 min. Cells were lysed and assayed for Rap1 activation with a pull-down assay. Precipitates (*top panel*) and total cell lysates (*bottom panel*) were analyzed by immunoblotting with anti-Rap1 mAb. *pAb*, polyclonal antibody.

protein expression (Fig. 1*C*), although increases in PKA activity after Fsk and 8-CPT-cAMP stimulation were effectively inhibited by the same concentrations of these agents (Fig. 1*D*). These data suggested that cAMP-induced c-IAP2 expression is predominantly regulated by PKA-independent pathways in colon epithelial cells. Subsequent studies were designed to examine this possibility.

cAMP Stimulates c-IAP2 Promoter Activity through Phosphorylation of CREB—Our previous data indicated that a CRE in the c-IAP2 promoter region is necessary for induction by cAMP (12), suggesting that CREB may be a prominent factor in controlling cAMP-dependent c-IAP2 transcription. To test this idea directly, we performed co-transfections with a minimal c-IAP2 transcriptional reporter that contains the proximal CRE region and is fully responsive to cAMP stimulation (12) and an expression vector encoding one of two dominant negative mutants of CREB, KCREB or CREB S133A. KCREB forms an inactive dimer with endogenous CREB and blocks its ability to bind to CRE (28). CREB S133A contains a serine to alanine mutation at position 133 that blocks phosphorylation of the mutant CREB and thus its ability to initiate CRE-dependent transcription (29). Both dominant negative forms of CREB abrogated increased c-IAP2 promoter activity induced by 8-CPT-cAMP (Fig. 2*A*) and CTX (data not shown), whereas co-transfection with wild-type CREB showed a slight, albeit not significant, increase in c-IAP2 promoter activity compared with vector-transfected control. Furthermore, consistent with its functional importance, endogenous CREB was phosphorylated in response to treatment of T84 cells with Fsk or 8-CPT-cAMP, whereas ATF-2 and CCAAT/enhancer-binding protein, other transcriptional factors that bind to CRE, were only minimally phosphorylated under these conditions (Fig. 2*B* and data not shown). Together these data indicate that phosphorylated CREB plays an essential role for c-IAP2 gene transcription in response to increases in cAMP.

CREB Phosphorylation Is Mediated by ERK1/2 and p38 MAPK—Phosphorylation of CREB is required for its transcriptional activation (30). Although PKA is an important kinase for CREB phosphorylation, we found that in T84 cells the PKA inhibitors H89 and (R_p)-cAMPS only slightly suppressed its cAMP-dependent phosphorylation (Fig. 2*B*). Therefore, we hypothesized that in this system other kinases, such as p90RSK, a kinase downstream of ERK1/2 (31), and MSK1, a kinase downstream of ERK1/2 and p38 MAPK (32), both of which can phosphorylate CREB (33), might participate in the phosphorylation of CREB in response to increases in cAMP. We found that both p90RSK and MSK1 were phosphorylated after stimulation with 8-CPT-cAMP (Fig. 3) and Fsk (data not shown). Phosphorylation of p90RSK promoted by 8-CPT-cAMP was inhibited by the MEK1/2 inhibitor U0126 (10 μM), while it was slightly, but not significantly, increased by the p38 MAPK inhibitor SB202190. 8-CPT-cAMP-promoted phosphorylation of MSK1 was inhibited moderately by both U0126 and SB202190 and more strongly by the combination of these agents (Fig. 3). The PKA inhibitors (R_p)-cAMPS (Fig. 3) and H89 (data not shown) did not affect Fsk- or 8-CPT-cAMP-stimulated phosphorylation of p90RSK or MSK1. These results suggest that cAMP activates p90RSK through ERK1/2 and

MSK1 through ERK1/2 and p38 MAPK in T84 cells and that activation of these kinases occurs independently of PKA.

Importantly CREB phosphorylation promoted by 8-CPT-cAMP (Fig. 3) or Fsk (data not shown) was significantly suppressed by U0126 or SB202190 alone, and this suppression was even more pronounced after addition of both inhibitors. Addition of (R_p)-cAMPS, which by itself only minimally decreased CREB phosphorylation (Fig. 2, *B* and 3, *lane b*), together with U0126 and SB202190 caused only modest and not significant further inhibition beyond that produced by the latter agents (Fig. 3, *lanes e* and *f*). Similar results were obtained by using other inhibitors for ERK1/2 and p38 MAPK, *i.e.* PD98059 and SB203850, respectively (data not shown). These data suggest that ERK1/2 and p38 MAPK are involved in the cAMP-dependent phosphorylation of CREB.

cAMP Activates ERK1/2 and p38 MAPK in T84 Cells—Because the results in Fig. 3 suggested the involvement of ERK1/2 and p38 MAPK in the phosphorylation of p90RSK and MSK1, we directly examined the activation of ERK1/2 and p38 MAPK in response to agents that raise cAMP levels. Treatment of T84 cells with PGE_2, Fsk, or 8-CPT-cAMP enhanced phosphorylation of ERK1/2 and p38 MAPK within 30 min as did TNFα as a positive control (Fig. 4*A*). Furthermore *in vitro* kinase assays demonstrated that increased phosphorylation of ERK1/2 and p38 MAPK after 8-CPT-cAMP stimulation was accompanied by activation of these kinases. Thus, activated-ERK1/2 or p38 MAPK immunoprecipitated from 8-CPT-cAMP-stimulated cell lysates showed an increased ability, relative to control cells, to phosphorylate their respective substrates, Elk or ATF-2 fusion proteins (Fig. 4, *B* and *C*). Increased ERK1/2 kinase activity was completely inhibited by treatment with U0126 but was insensitive to PKA inhibitors (Fig. 4*B*), documenting further that ERK1/2 activation is PKA-independent in T84 cells. In contrast, in CHO cells ERK1/2 activation by cAMP is a PKA-dependent event because H89 inhibited ERK1/2 phosphorylation induced by 8-CPT-cAMP stimulation (Fig. 4*E*), a finding consistent with prior reports (34). The PKA inhibitors also failed to inhibit the cAMP-dependent increase in p38 MAPK activity (Fig. 4*C*). Taken together, these results support the conclusion that increases in cAMP activate both ERK1/2 and p38 MAPK in T84 cells, and these activations appear to occur independently of PKA.

In addition to PKA, another recently recognized effector of cAMP action is Epac, a guanine nucleotide exchange factor for the small GTPase Rap, which is able to regulate ERK1/2 activity in some cells (35, 36). Because our results showed that cAMP-promoted ERK1/2 activation is a PKA-independent event, we examined the ability of 8-CPT-2′-*O*-Me-cAMP, a specific activator of Epac that activates Rap1 in CHO, PC12, and human embryonic kidney 293T cells (34), to stimulate ERK1/2 activation in T84 cells. We found that 8-CPT-2′-*O*-Me-cAMP failed to activate ERK1/2 and p38 MAPK in these cells (Fig. 4, *D* and *E*), although as a positive control, this analog was able to activate Rap1 (Fig. 4*F*), consistent with the conclusion that cAMP-promoted ERK1/2 activation in T84 cells occurs via an Epac-independent pathway.

cAMP Induces c-IAP2 Expression through the Activation of ERK1/2 and p38 MAPK—We next examined the involvement of ERK1/2 and p38 MAPK in cAMP-dependent transcriptional activation of the c-IAP2 gene. Stimulation of c-IAP2 promoter activity by CTX and 8-CPT-cAMP (see Fig. 1*A*) was significantly diminished by adding the MEK1/2 inhibitor U0126 and the p38 MAPK inhibitor SB202190, and this inhibition was even greater by combined treatment with both inhibitors (Fig. 5*A*). Consistent with this, increased c-IAP2 protein expression after stimulation with CTX and 8-CPT-cAMP was also markedly inhibited by the combination of inhibitors of MEK1/2 and p38 MAPK (Fig. 5*B*). Addition of (R_p)-cAMPS yielded no significant further inhibition of c-IAP2 expression, providing addi-

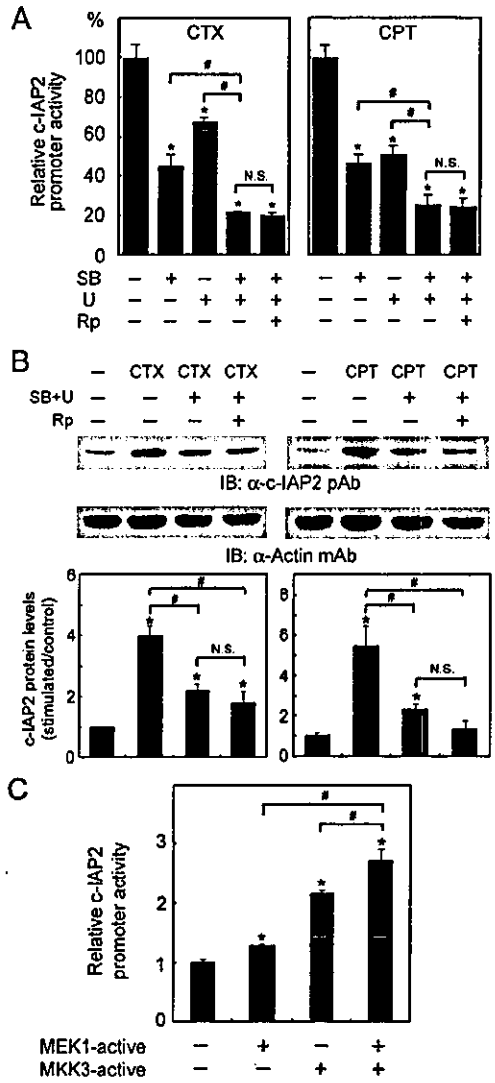

FIG. 5. **cAMP induces c-IAP2 protein expression through ERK1/2 and p38 MAPK activation.** *A*, T84 cells, transfected with pGL3-c-IAP2-Luc and pSV40-RL-Luc, were treated for 1 h with (R_p)-cAMPS (*Rp*, 100 μM), SB202910 (*SB*, 20 μM), and U0126 (*U*, 10 μM) alone or in combination and stimulated for 12 h with CTX (250 ng/ml) or 6 h with 8-CPT-cAMP (*CPT*, 100 μM). Cell extracts were assayed by a dual luciferase assay. Results represent relative promoter activity compared with CTX- or CPT-treated cells without inhibitors as 100% and are mean ± S.E. (n = 3; *, $p < 0.05$ *versus* CTX- or CPT-treated cells without inhibitors; #, $p < 0.05$ relative to cells treated with either of the inhibitors alone; *N.S.*, not significant). *B*, T84 cells were treated for 1 h with (R_p)-cAMPS (*Rp*, 100 μM), SB202910 (*SB*, 20 μM), and/or U0126 (*U*, 10 μM) as indicated and incubated for 12 h with CTX (250 ng/ml) or 6 h with 8-CPT-cAMP (*CPT*, 100 μM). Cells were lysed in SDS sample buffer, and proteins were analyzed by immunoblotting with the indicated antibodies. The *lower graphs* show densitometric results of the respective blots normalized against actin levels and expressed relative to unstimulated controls without inhibitors and are mean ± S.E. (n = 3; *, $p < 0.05$ *versus* untreated controls; #, $p < 0.05$; *N.S.*, not significant). *C*, T84 cells were transfected with pUSE-MEK1 (S218D/S222D) (*MEK1-active*) and/or pBabeHygro-MKK3A (*MKK3-active*), pGL3-c-IAP2-Luc, and pSV40-RL-Luc and incubated for 12 h. Cell extracts were assayed by a dual luciferase assay. Results represent relative increases compared with vector-transfected controls and are mean ± S.E. (n = 3; *, $p < 0.05$ *versus* vector-transfected cells; #, $p < 0.05$). *IB*, immunoblot; *pAb*, polyclonal antibody.

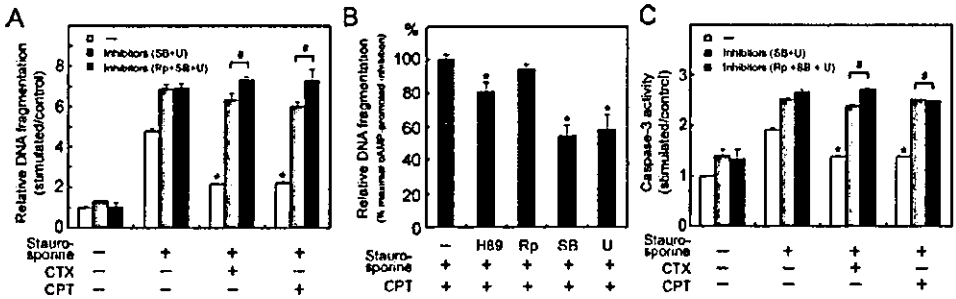

FIG. 6. **cAMP regulates apoptosis through ERK1/2 and p38 MAPK.** T84 cells were incubated for 1 h with H89 (10 μM), (R_p)-cAMPS (*Rp*, 100 μM), SB202910 (*SB*, 20 μM), and/or U0126 (*U*, 10 μM) as indicated followed by further incubation for 1 h with CTX (250 ng/ml) or 8-CPT-cAMP (*CPT*, 100 μM). Cells were stimulated with staurosporine (200 nM) for 12 h, and oligonucleosome release into the cytoplasm was assayed by enzyme-linked immunosorbent assay (*A* and *B*), or for 6 h, and caspase-3 activity was assayed by enzyme-linked immunosorbent assay (*C*). *A* and *C*, results represent relative increases compared with untreated cells without inhibitors, respectively, and are mean ± S.E. (n = 3; *, $p < 0.05$ *versus* staurosporine-treated cells without CTX or CPT stimulation; #, $p < 0.05$). *B*, results represent relative levels of 8-CPT-cAMP-mediated inhibition of DNA fragmentation induced by staurosporine compared with CPT- and staurosporine-treated cells without inhibitors as 100% and are shown as mean ± S.E. (n = 3; *, $p < 0.05$ *versus* CPT- and staurosporine-treated cells without inhibitors).

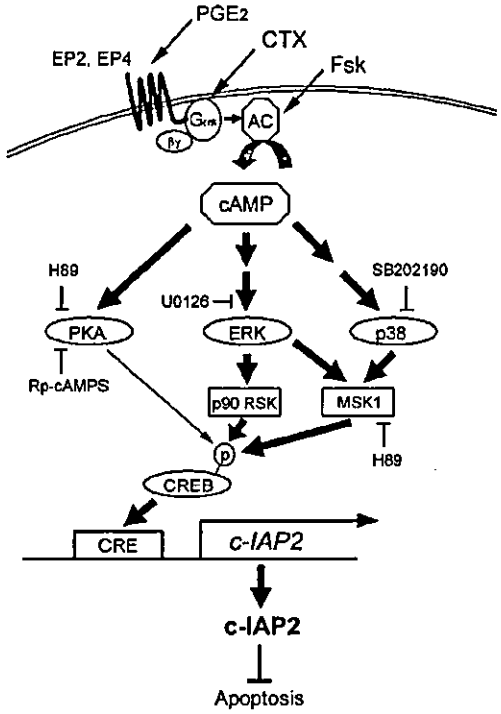

FIG. 7. **Model of cAMP-mediated c-IAP2 induction.** PGE_2-, CTX-, and Fsk-stimulated increases in cAMP activate PKA, ERK1/2, and p38 MAPK followed by p90RSK and MSK1 activation. The actions of cAMP on ERK1/2 and p38 MAPK activation are likely to be indirect as indicated in the figure with *two arrows*. CREB, phosphorylated in response to activation of p90RSK and MSK1, and to a lesser degree PKA, then induces c-IAP2 expression through CRE within the proximal c-IAP2 promoter region. c-IAP2 protein inhibits activated caspase-3 and apoptosis. *AC*, adenylyl cyclase.

tional support for the conclusion that PKA has a limited, if any, role in mediating cAMP-dependent c-IAP2 induction.

As an alternative approach to defining the role of ERK1/2 and p38 MAPK in the regulation of c-IAP2 expression, we performed co-transfections with a c-IAP2 promoter-reporter and expression vectors for dominant active forms of MEK1 and/or MKK3, which are potent activators of ERK1/2 and p38 MAPK, respectively (25, 37). Forced expression of active forms of MEK1 or MKK3 induced c-IAP2 promoter activity, which was further enhanced by co-transfection with both expression plasmids (Fig. 5*C*). Based on these data, we conclude that ERK1/2 and p38 MAPK play a pivotal role in the cAMP-promoted induction of c-IAP2 via increased phosphorylation of CREB.

cAMP Regulates Apoptosis in Colon Epithelial Cells through ERK1/2 and p38 MAPK—To assess the biological significance of the involvement of ERK1/2 and p38 MAPK in the c-IAP2 induction stimulated by cAMP, we assayed T84 cells for apoptosis. Treatment of T84 cells with CTX or 8-CPT-cAMP inhibited apoptosis induced by staurosporine as assessed by quantitative analysis of DNA fragmentation. This inhibition was abrogated by adding a combination of inhibitors of ERK1/2 and p38 MAPK (Fig. 6*A*). When we examined these inhibitors individually, U0126 and SB202190 as well as H89 but not (R_p)-cAMPS, each significantly blunted the 8-CPT-cAMP-promoted inhibition of staurosporine-induced apoptosis (Fig. 6*B*). The difference between the responses to H89 and (R_p)-cAMPS might relate to the ability of H89 to inhibit not only PKA but also MSK1 (38). U0126 and SB202190 also blocked the inhibition of caspase-3 activity produced by CTX or 8-CPT-cAMP treatment of T84 cells (Fig. 6*C*); this effect was not further enhanced by addition of (R_p)-cAMPS. These results are consistent with the action of c-IAP2 in binding to the active form of caspase-3 and thereby diminishing its activity (15) and with results of experiments shown above for the role of kinases other than PKA in regulation of c-IAP2 expression. Fig. 7 shows a model that summarizes these pathways.

DISCUSSION

Apoptosis is a complex cellular process that is regulated by a balance of stimulatory and inhibitory pathways. The ability of cAMP to inhibit apoptosis might result from a blockade of proapoptotic pathways, a stimulation of antiapoptotic pathways, or a combination thereof. While some of the proapoptotic members of the Bcl-2 family, such as BAD, have been reported to be phosphorylated and inactivated by PKA, thereby resulting in inhibition of apoptosis (40–43), we recently identified an alternative mechanism for cAMP-mediated antiapoptosis: an inhibition of apoptosis in intestinal epithelial cells by agonists that increase cAMP and induce c-IAP2 via a CRE in the c-IAP2 promoter (12). We showed that c-IAP2 induction by increases in cAMP levels inhibits apoptosis that occurs in response to anti-Fas antibody (extrinsic apoptotic pathway) or staurosporine (intrinsic apoptotic pathway). The results thus suggested a novel mechanism for the cancer-chemopreventive effect of nonsteroidal anti-inflammatory drugs, which inhibit cyclooxygenases and decrease PGE_2 synthesis (12).

In the current studies, we have identified new aspects of the

signal transduction pathway by which increases in cAMP induce c-IAP2 expression in colon cancer cells (Fig. 7). The data show that CREB phosphorylation is a key step but that the phosphorylation appears to occur by kinases other than the expected involvement of PKA. Activation of p90RSK and MSK1, which follow ERK1/2 and p38 MAPK activation, appears to be involved in both CREB phosphorylation and c-IAP2 induction. The current data also suggest that agents that raise intracellular cAMP and induce c-IAP2 expression in T84 cells do not appear to act via ATF-2 and CCAAT/enhancer-binding protein, other transcriptional factors that bind to CRE, because we found minimal phosphorylation of ATF-2 and CCAAT/enhancer-binding protein after cAMP treatment.

Conventional ideas emphasize that cAMP-mediated transcriptional responses involve the ability of PKA to phosphorylate CREB (30). However, the data shown here provide evidence for an alternative mechanism whereby cAMP promotes phosphorylation of CREB through ERK1/2 and p38 MAPK and perhaps other protein kinases as well. Previous data have implicated a role for p90RSK in the phosphorylation of CREB promoted by certain growth factors (44, 45). Several of our results imply a limited involvement of PKA: 1) two different PKA inhibitors (H89 and (R_p)-cAMPS) used at concentrations that block PKA activity yielded only minimal inhibition of CREB phosphorylation, c-IAP2 promoter activity, and c-IAP2 protein levels, and 2) addition of (R_p)-cAMPS along with inhibitors of ERK1/2 and p38 MAPK did not cause greater inhibition of cAMP-induced c-IAP2 induction or abrogation of inhibition of apoptosis or caspase activation by cAMP despite inhibition of PKA activity. Thus, the current results emphasize a role for ERK1/2 and p38 MAPK in cAMP-mediated induction of c-IAP2. However, because H89 and (R_p)-cAMPS had some ability to decrease cAMP-promoted CREB phosphorylation and c-IAP2 promoter activity, PKA might contribute in a limited way to CRE-dependent transcription through CREB phosphorylation.

cAMP is involved in multiple cellular processes that are thought to be mediated by PKA and Epac (46). Increases in cAMP activate ERK1/2 through PKA in CHO, PC12, and human embryonic kidney 293T cells (34) or through Epac-Rap1 in primary kidney cells (35), while ERK1/2 is inhibited by increases in cAMP in NIH 3T3 cells (34) and C6 rat glioma cells (47). Moreover an increase in cAMP levels promoted by thyroid-stimulating hormone stimulation activates p38 MAPK through PKA in thyroid-stimulating hormone receptor-overexpressing CHO cells (48), while cAMP activates p38 MAPK in a PKA-independent manner in Th2 effector T cells (49). Here we show that increases in cAMP induce ERK1/2 and p38 MAPK activation in colon epithelial cells through PKA- and Epac-independent pathways, suggesting involvement of alternative mechanisms of MAPK activation.

MAPKs regulate cellular activities ranging from gene expression, mitosis, motility, and metabolism to apoptosis. The ability of ERK1/2 to regulate cell proliferation has led to the exploration of inhibitors of ERK1/2 as possible anticancer agents (50, 51). The potential role of p38 MAPK in cancer chemotherapy has also been considered, although p38 MAPK inhibitors have primarily been tested for inflammatory disorders (52, 53). In fact, inhibition of p38 MAPK promotes cell death of UV radiation-treated melanoma cells (54) and TNFα-treated myelomonocytic cells (55). Our results emphasize the function of ERK1/2 and p38 MAPK in inhibition of apoptosis through c-IAP2 induction and suggest a mechanism that may contribute to actions of those kinases in cell death.

CREB has been reported to regulate a number of target genes related to tumorigenesis and to cell survival (56, 57), including cyclin D1 or *BRCA1* (30). Our findings emphasize the biological significance of CREB phosphorylation as a key event in the induction of c-IAP2 via multiple protein kinases in addition to PKA. The data also suggest that kinase inhibitors, other than inhibitors of PKA, might be able to blunt cAMP-promoted antiapoptosis. As an alternative approach, one might consider a CRE decoy system in which a decoy oligodeoxynucleotide carrying a CRE can be used to inhibit CRE-directed gene transcription and tumor growth without affecting normal cell growth (39).

Acknowledgment—We thank Dr. Peiqing Sun for kindly providing pBabeHygro-MKK3A.

REFERENCES

1. Reed, J. C. (1999) *J. Clin. Oncol.* **17**, 2941–2953
2. Boucher, M. J., Duchesne, C., Laine, J., Morisset, J., and Rivard, N. (2001) *Biochem. Biophys. Res. Commun.* **285**, 207–216
3. Garcia-Bermejo, L., Perez, C., Vilaboa, N. E., de Blas, E., and Aller, P. (1998) *J. Cell Sci.* **111**, 637–644
4. Baumann, C. A., Badamchian, M., and Goldstein, A. L. (1997) *Mech. Ageing Dev.* **94**, 85–101
5. Tortora, G., and Ciardiello, F. (2002) *Ann. N. Y. Acad. Sci.* **968**, 139–147
6. Tortora, G., and Ciardiello, F. (2002) *Clin. Cancer Res.* **8**, 303–304
7. Cho, Y. S., Kim, M. K., Tan, L., Srivastava, R., Agrawal, S., and Cho-Chung, Y. S. (2002) *Clin. Cancer Res.* **8**, 607–614
8. Coleman, R. A., Smith, W. L., and Narumiya, S. (1994) *Pharmacol. Rev.* **46**, 205–229
9. Rigas, B., Goldman, I. S., and Levine, L. (1993) *J. Lab. Clin. Med.* **122**, 518–523
10. Chan, T. A. (2002) *Lancet Oncol.* **3**, 166–174
11. Leahy, K. M., Ornberg, R. L., Wang, Y., Zweifel, B. S., Koki, A. T., and Masferrer, J. L. (2002) *Cancer Res.* **62**, 625–631
12. Nishihara, H., Kizaka-Kondoh, S., Insel, P. A., and Eckmann, L. (2003) *Proc. Natl. Acad. Sci. U. S. A.* **100**, 8921–8926
13. Crook, N. E., Clem, R. J., and Miller, L. K. (1993) *J. Virol.* **67**, 2168–2174
14. Birnbaum, M. J., Clem, R. J., and Miller, L. K. (1994) *J. Virol.* **68**, 2521–2528
15. Deveraux, Q. L., and Reed, J. C. (1999) *Genes Dev.* **13**, 239–252
16. Tamm, I., Kornblau, S. M., Segall, H., Krajewski, S., Welsh, K., Kitada, S., Scudiero, D. A., Tudor, G., Qui, Y. H., Monks, A., Andreeff, M., and Reed, J. C. (2000) *Clin. Cancer Res.* **6**, 1796–1803
17. Hoffman, W. H., Biade, S., Zilfou, J. T., Chen, J., and Murphy, M. (2002) *J. Biol. Chem.* **277**, 3247–3257
18. Salvesen, G. S., and Duckett, C. S. (2002) *Nat. Rev. Mol. Cell. Biol.* **3**, 401–410
19. Roy, N., Deveraux, Q. L., Takahashi, R., Salvesen, G. S., and Reed, J. C. (1997) *EMBO J.* **16**, 6914–6925
20. Dierlamm, J., Baens, M., Wlodarska, I., Stefanova-Ouzounova, M., Hernandez, J. M., Hossfeld, D. K., De Wolf-Peeters, C., Hagemeijer, A., Van den Berghe, H., and Marynen, P. (1999) *Blood* **93**, 3601–3609
21. Deveraux, Q. L., Roy, N., Stennicke, H. R., Van Arsdale, T., Zhou, Q., Srinivasula, S. M., Alnemri, E. S., Salvesen, G. S., and Reed, J. C. (1998) *EMBO J.* **17**, 2215–2223
22. Chu, Z. L., McKinsey, T. A., Liu, L., Gentry, J. J., Malim, M. H., and Ballard, D. W. (1997) *Proc. Natl. Acad. Sci. U. S. A.* **94**, 10057–10062
23. Ueda, T., Akiyama, N., Sai, H., Oya, N., Noda, M., Hiraoka, M., and Kizaka-Kondoh, S. (2001) *FEBS Lett.* **491**, 40–44
24. Webster, J. C., Huber, R. M., Hanson, R. L., Collier, P. M., Haws, T. F., Mills, J. K., Burn, T. C., and Allegretto, E. A. (2002) *Endocrinology* **143**, 3866–3874
25. Wang, W., Chen, J. X., Liao, R., Deng, Q., Zhou, J. J., Huang, S., and Sun, P. (2002) *Mol. Cell. Biol.* **22**, 3389–3403
26. Bastien, L., Sawyer, N., Grygorczyk, R., Metters, K. M., and Adam, M. (1994) *J. Biol. Chem.* **269**, 11873–11877
27. Belley, A., and Chadee, K. (1999) *Gastroenterology* **117**, 1352–1362
28. Walton, K. M., Rehfuss, R. P., Chrivia, J. C., Lochner, J. E., and Goodman, R. H. (1992) *Mol. Endocrinol.* **6**, 647–655
29. Gonzalez, G. A., and Montminy, M. R. (1989) *Cell* **59**, 675–680
30. Mayr, B., and Montminy, M. (2001) *Nat. Rev. Mol. Cell. Biol.* **2**, 599–609
31. Frodin, M., and Gammeltoft, S. (1999) *Mol. Cell. Endocrinol.* **151**, 65–77
32. Deak, M., Clifton, A. D., Lucocq, L. M., and Alessi, D. R. (1998) *EMBO J.* **17**, 4426–4441
33. Xing, J., Kornhauser, J. M., Xia, Z., Thiele, E. A., and Greenberg, M. E. (1998) *Mol. Cell. Biol.* **18**, 1946–1955
34. Enserink, J. M., Christensen, A. E., de Rooij, J., van Triest, M., Schwede, F., Genieser, H. G., Doskeland, S. O., Blank, J. L., and Bos, J. L. (2002) *Nat. Cell Biol.* **4**, 901–906
35. Laroche-Joubert, N., Marsy, S., Michelet, S., Imbert-Teboul, M., and Doucet, A. (2002) *J. Biol. Chem.* **277**, 18598–18604
36. Stork, P. J., and Schmitt, J. M. (2002) *Trends Cell Biol.* **12**, 258–266
37. Mansour, S. J., Matten, W. T., Hermann, A. S., Candia, J. M., Rong, S., Fukasawa, K., Vande Woude, G. F., and Ahn, N. G. (1994) *Science* **265**, 966–970
38. Davies, S. P., Reddy, H., Caivano, M., and Cohen, P. (2000) *Biochem. J.* **351**, 95–105
39. Cho, Y. S., Kim, M. K., Cheadle, C., Neary, C., Park, Y. G., Becker, K. G., and Cho-Chung, Y. S. (2002) *Proc. Natl. Acad. Sci. U. S. A.* **99**, 15626–15631
40. Harada, H., Becknell, B., Wilm, M., Mann, M., Huang, L. J., Taylor, S. S., Scott, J. D., and Korsmeyer, S. J. (1999) *Mol. Cell* **3**, 413–422
41. Tan, Y., Demeter, M. R., Ruan, H., and Comb, M. J. (2000) *J. Biol. Chem.* **275**,

25865–25869
42. Lizcano, J. M., Morrice, N., and Cohen, P. (2000) *Biochem. J.* **349**, 547–557
43. Datta, S. R., Katsov, A., Hu, L., Petros, A., Fesik, S. W., Yaffe, M. B., and Greenberg, M. E. (2000) *Mol. Cell* **6**, 41–51
44. Xing, J., Ginty, D. D., and Greenberg, M. E. (1996) *Science* **273**, 959–963
45. Ginty, D. D., Bonni, A., and Greenberg, M. E. (1994) *Cell* **77**, 713–725
46. Kopperud, R., Krakstad, C., Selheim, F., and Doskeland, S. O. (2003) *FEBS Lett.* **546**, 121–126
47. Wang, L., Liu, F., and Adamo, M. L. (2001) *J. Biol. Chem.* **276**, 37242–37249
48. Pomerance, M., Abdullah, H. B., Kamerji, S., Correze, C., and Blondeau, J. P. (2000) *J. Biol. Chem.* **275**, 40539–40546
49. Chen, C. H., Zhang, D. H., LaPorte, J. M., and Ray, A. (2000) *J. Immunol.* **165**, 5597–5605
50. Sebolt-Leopold, J. S. (2000) *Oncogene* **19**, 6594–6599
51. Johnson, G. L., and Lapadat, R. (2002) *Science* **298**, 1911–1912
52. Fan, M., and Chambers, T. C. (2001) *Drug Resist. Updat.* **4**, 253–267
53. English, J. M., and Cobb, M. H. (2002) *Trends Pharmacol. Sci.* **23**, 40–45
54. Ivanov, V. N., and Ronai, Z. (2000) *Oncogene* **19**, 3003–3012
55. Varghese, J., Chattopadhaya, S., and Sarin, A. (2001) *J. Immunol.* **166**, 6570–6577
56. Riccio, A., Ahn, S., Davenport, C. M., Blendy, J. A., and Ginty, D. D. (1999) *Science* **286**, 2358–2361
57. Bonni, A., Brunet, A., West, A. E., Datta, S. R., Takasu, M. A., and Greenberg, M. E. (1999) *Science* **286**, 1358–1362

THE JOURNAL OF BIOLOGICAL CHEMISTRY
Vol. 279, No. 4, Issue of January 23, pp. 2550–2558, 2004
Printed in U.S.A.

Nitric Oxide Induces Hypoxia-inducible Factor 1 Activation That Is Dependent on MAPK and Phosphatidylinositol 3-Kinase Signaling*

Received for publication, July 28, 2003, and in revised form, October 6, 2003
Published, JBC Papers in Press, November 4, 2003, DOI 10.1074/jbc.M308197200

Kenji Kasuno‡§, Satoshi Takabuchi¶‖, Kazuhiko Fukuda‖, Shinae Kizaka-Kondoh, Junji Yodoi‡§, Takehiko Adachi¶, Gregg L. Semenza‡‡, and Kiichi Hirota¶‖§§**

*From the ‡Human Stress Signal Research Center, National Institute of Advanced Industrial Science and Technology, IKEDA, Osaka, Japan 563-0053, the ¶Department of Anesthesia, Tazuke Kofukai Medical Research Institute Kitano Hospital, 2-4-20, Ohgimachi, Kita-ku, Osaka 530-8480, the §Institute for Virus Research and ‖Department of Anesthesia, Kyoto University Hospital, Kyoto University, Kyoto 606-8507, Japan, the **Department of Molecular Oncology, Kyoto University Graduate School of Medicine, Sakyo-ku, Kyoto 606-8507, Japan, and the ‡‡McKusick-Nathans Institute of Genetic Medicine, The Johns Hopkins University School of Medicine, Baltimore, Maryland 21287*

Hypoxia-inducible factor-1 (HIF-1) is a master regulator of cellular adaptive responses to hypoxia. Levels of the HIF-1α subunit increase under hypoxic conditions. Exposure of cells to certain nitric oxide (NO) donors also induces HIF-1α expression under nonhypoxic conditions. We demonstrate that exposure of cells to the NO donor NOC18 or *S*-nitrosoglutathione induces HIF-1α expression and transcriptional activity. In contrast to hypoxia, NOC18 did not inhibit HIF-1α hydroxylation, ubiquitination, and degradation, indicating an effect on HIF-1α protein synthesis that was confirmed by pulse labeling studies. NOC18 stimulation of HIF-1α protein and HIF-1-dependent gene expression was blocked by treating cells with an inhibitor of the phosphatidylinositol 3-kinase or MAPK-signaling pathway. These inhibitors also blocked NOC18-induced phosphorylation of the translational regulatory proteins 4E-BP1, p70 S6 kinase, and eIF-4E, thus providing a mechanism for the modulation of HIF-1α protein synthesis. In addition, expression of a dominant-negative form of Ras significantly suppressed HIF-1 activation by NOC18. We conclude that the NO donor NOC18 induces HIF-1α synthesis under conditions of NO formation during normoxia and that hydroxylation of HIF-1α is not regulated by NOC18.

Hypoxia induces a series of adaptive physiological responses (1). At the cellular level, the adaptation involves a switch of energy metabolism from oxidative phosphorylation to anaerobic glycolysis, increased glucose uptake, and the expression of stress proteins related to cell survival or death (2). At the molecular level, the adaptation involves changes in mRNA transcription and mRNA stability (2, 3). One of the most important transcription factors that activates the expression of oxygen-regulated genes including vascular endothelial growth factor (VEGF)[1] and inducible nitric-oxide synthase is hypoxia-inducible factor 1 (HIF-1) (4–6). VEGF is a potent angiogenic and vascular permeability factor that plays critical roles in both physiological and pathological angiogenesis (7). Recently, the expression of VEGF in response to heregulin-induced activation of the HER2/neu receptor tyrosine kinase in breast cancer cells (8), IGF-1 stimulation of colon cancer cells (9), and insulin treatment of retinal pigment epithelial cells (10) was shown to be mediated by HIF-1 via the phosphatidylinositol 3-kinase (PI3K) and mitogen-activated protein kinase (MAPK) pathways. Thus, HIF-1 regulates both hypoxia- and growth factor-induced VEGF expression.

HIF-1 is a heterodimer composed of a constitutively expressed β subunit (HIF-1β) and an inducibly expressed α subunit (HIF-1α) (4). The regulation of HIF-1 activity occurs at multiple levels *in vivo* (11). Among these, the mechanisms regulating HIF-1α protein expression and transcriptional activity have been most extensively analyzed. The von Hippel-Lindau tumor suppressor protein (VHL) has been identified as the HIF-1α-binding component of a ubiquitin-protein ligase that targets HIF-1α for proteasomal degradation in nonhypoxic cells (12–15). Under hypoxic conditions, the hydroxylation of specific proline and asparagine residues in HIF-1α is inhibited due to substrate (O_2) limitation, resulting in HIF-1α protein stabilization and transcriptional activation (14, 16, 17). The iron chelator deferrioxamine (DFX) inhibits the prolyl and asparaginyl hydroxylases, which contain Fe^{2+} at their catalytic sites, causing HIF-1α stabilization and transactivation under normoxic conditions (12, 13).

Signaling via the HER2/neu and IGF-1 receptor tyrosine kinases induces HIF-1 expression by an independent mechanism. HER2/neu activation increases the rate of HIF-1α protein synthesis via PI3K and the downstream serine-threonine kinases AKT (protein kinase B) and FKBP/rapamycin-associated protein (FRAP; also known as mammalian target of rapamycin (mTOR)) (8). IGF-1-induced HIF-1α synthesis is dependent upon both the PI3K and MAPK pathways (10). FRAP/mTOR phosphorylates and activates the translational

* This work was supported in part by a grant-in-aid for scientific research on priority areas "Cancer" from the Ministry of Education, Culture, Sports, Science and Technology (to K. H.). The costs of publication of this article were defrayed in part by the payment of page charges. This article must therefore be hereby marked "*advertisement*" in accordance with 18 U.S.C. Section 1734 solely to indicate this fact.

§§ To whom correspondence should be addressed. Tel.: 81-6-6312-8831; Fax: 81-6-6361-8867; E-mail: khirota@kuhp.kyoto-u.ac.jp.

[1] The abbreviations used are: VEGF, vascular endothelial growth factor; HIF-1, hypoxia-inducible factor 1; GLUT1, glucose transporter 1; MAPK, mitogen-activated protein kinase; PI3K, phosphatidylinositol 3-kinase; NO, nitric oxide; eIF-4E, eukaryotic initiation factor; 4E-BP1, eIF-4E-binding protein 1; FRAP, FKBP/rapamycin-associated protein; mTOR, mammalian target of rapamycin; VHL, von Hippel-Lindau; HRE, hypoxia-responsive element; DFX, desferrioxamine; TAD, transactivation domain; HA, hemagglutinin; GST, glutathione *S*-transferase; GSNO, *S*-nitrosoglutathione; SNP, sodium nitroprusside; CHX, cycloheximide; RT, reverse transcriptase; PBS, phosphate-buffered saline; X-gal, 5-bromo-4-chloro-3-indolyl-β-D-galactopyranoside; NLS, nuclear localization signal; ERK, extracellular signal-regulated kinase; MEK, mitogen-activated protein kinase/extracellular signal-regulated kinase kinase; CREB, cAMP-response element-binding protein; E1, ubiquitin-activating enzyme; E2, ubiquitin carrier protein.

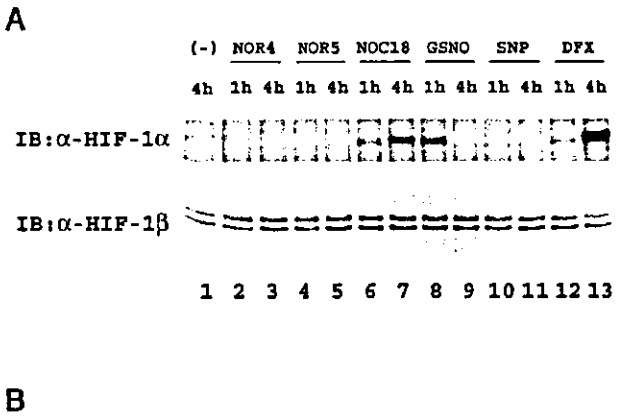

FIG. 1. **Effect of NO donors on HIF-1α levels in HEK293 cells.** *A*, HEK293 cells were exposed to 500 μM NOR4 (*lanes 2* and *3*), 500 μM NOR5 (*lanes 4* and *5*), 500 μM NOC18 (*lanes 6* and *7*), 500 μM GSNO (*lanes 8* and *9*), 100 μM SNP (*lanes 10* and *11*), or 100 μM DFX (*lanes 12* and *13*) for the indicated periods, and whole cell lysates were subject to an immunoblot (*IB*) assay for HIF-1α (*upper panel*) or HIF-1β (*lower panel*) protein expression. *B*, HEK293 cells were exposed to the indicated doses of NOC18 or GSNO prior to immunoblot analysis of whole cell lysates using monoclonal antibodies specific for HIF-1α (*top*) or HIF-1β protein (*bottom*). *C*, comparison of kinetics of HIF-1α induction by NOC12 and NOC18. Cells were exposed to 500 μM NOC12 (*top, lanes 2–5*), 500 μM NOC18 (*top, lanes 6–9*), 40 μM NOC12 (*bottom, lanes 2–4*), or 500 μM NOC18 (*bottom, lanes 5–7*) for 30 min to 8 h prior to immunoblot analysis.

regulatory proteins eukaryotic initiation factor 4E (eIF-4E)-binding protein 1 (4E-BP1) and p70 S6 kinase ($p70^{S6K}$). Phosphorylation of 4E-BP1 disrupts its inhibitory interaction with eIF-4E, whereas activated $p70^{S6K}$ phosphorylates the 40 S ribosomal protein S6. The effect of HER2/neu signaling on translation of HIF-1α protein is dependent upon the presence of the 5′-untranslated region of HIF-1α mRNA (8).

Nitric oxide (NO) is known to mediate many physiological and pathological functions including vascular dilatation, cytotoxicity mediated by activated macrophages, and cGMP formation following glutamate receptor activation in neurons (18).

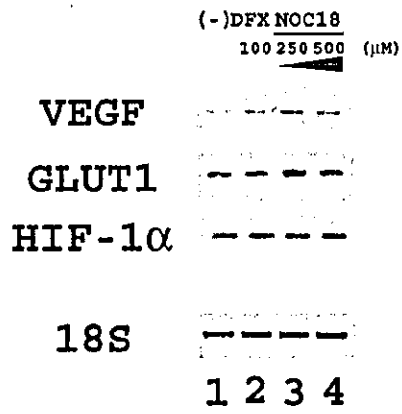

FIG. 2. **Effect of NOC18 on expression of HIF-1 target genes.** HEK293 cells were treated with NOC18 or DFX for 24 h, and total RNA was isolated. Expression of VEGF, GLUT1, and HIF-1α mRNA and 18 S rRNA was analyzed by RT-PCR.

NO has also been implicated in pathological conditions such as destruction of tumor cells by macrophages, rheumatoid arthritis, and focal brain ischemia. There are several reports demonstrating that exposure of cells to certain NO donors or gaseous NO modulates HIF-1 activity (19–23). *S*-nitrosoglutathione (GSNO) or NOC18 induces HIF-1 activity under nonhypoxic conditions (22). In contrast, sodium nitroprusside (SNP) inhibits hypoxia-induced HIF-1 activation (19–21). However, the molecular mechanisms that regulate HIF-1α expression and transactivation in response to NO donors are poorly defined. In this study, we found that NOC18 induces HIF-1 activity by increasing HIF-1α protein synthesis via PI3K- and MAPK-dependent pathways.

EXPERIMENTAL PROCEDURES

Cell Culture and Reagents—Hep3B cells, HEK293 cells, and HCT116 cells were maintained in minimal essential medium with Earle's salts, Dulbecco's modified Eagle's medium, and McCoy's 5A medium, respectively, supplemented with 10% fetal bovine serum and 100 units/ml penicillin, and 100 μg/ml streptomycin. Human umbilical vein endothelial cells were obtained from Kurabo (Osaka, Japan) and cultured with HuMedia-EG2 (Kurabo). DFX, the thiol-dependent NO releaser GSNO, and *N*-acetyl cysteine were obtained from Sigma. The spontaneous NO releasers NOR4 (half-life, 60 min), NOR5 (half-life, 20 h), NOC12 (half-life, 100 min), and NOC18 (half-life, 21 h) were obtained from Dojindo (Kumamoto, Japan). Cycloheximide (CHX), SNP, wortmannin, genistein, LY294002, PD98059, and rapamycin were obtained from Calbiochem.

Plasmid Constructs—Expression vectors pGAL4/HIF-1α (531–826), pGAL4/HIF-1α(531–575), pGAL4/HIF-1α(726–826), and pGAL4/HIF-1α(786–826) were described previously (24). Plasmid p2.1 contains a 68-bp hypoxia response element (HRE) from the *ENO1* gene inserted upstream of an SV40 promoter in the luciferase reporter plasmid pGL2-Promoter (Promega), and p2.4 contains a mutation in the HRE (24, 25). Plasmid pVEGF-KpnI contains nucleotides −2274 to +379 of the human VEGF gene inserted into the luciferase reporter pGL2-Basic (Promega) (26). The reporter GAL4E1bLuc contains five copies of a GAL4 binding site upstream of a TATA sequence and firefly luciferase coding sequences (24). A FLAG-tagged dominant negative form of HIF-1α pCMV-3XFLAG-HIF-1αΔNBΔAB was generated based on pCEP4-HIF-1αΔNBΔAB (27). The expression plasmid pCH-NLS-HIF1α(548–603)-LacZ was described elsewhere (28). Plasmids encoding p85Δ, a dominant-negative form of the PI3K p85 regulatory subunit, and a kinase-dead form of Akt were gifts from Dr. Wataru Ogawa (Kobe University, Kobe, Japan) (29, 30). Plasmid encoding a dominant negative form of Ras (31) was a generous gift from Dr. Kaikobad Irani (The Johns Hopkins University, Baltimore, MD).

Hypoxic Treatment—Tissue culture dishes were transferred to a modular incubator chamber (Billups-Rothenberg, Del Mar, CA), which was flushed with 1% O_2, 5% CO_2, 94% N_2, sealed, and placed at 37 °C.

Immunoblot Assays—Whole cell lysates were prepared by incubating cells for 30 min in cold radioimmune precipitation assay buffer containing 2 mM dithiothreitol, 1 mM $NaVO_3$, and Complete protease inhibitor

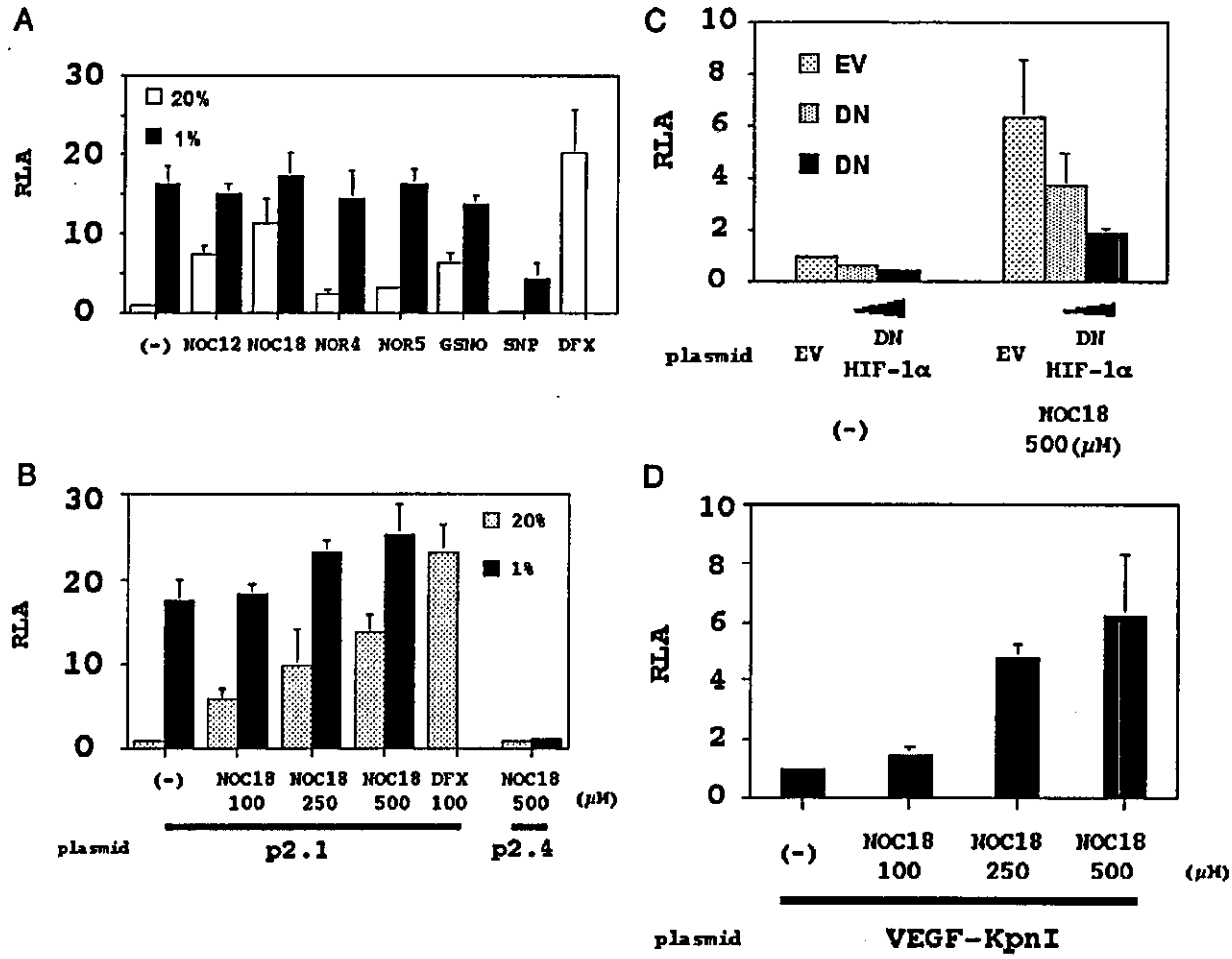

FIG. 3. **Effect of NO donors on HRE-dependent gene expression.** HEK293 cells were transfected with pTK-RL encoding *Renilla* luciferase and one of the following plasmids encoding firefly luciferase: HRE reporter p2.1 (*A–C*), mutant HRE reporter p2.4 (*B*), or VEGF promoter reporter pVEGF-KpnI-Luc (*D*). Cells were exposed to 20 or 1% O_2 with or without NO donors for 16 h and then harvested for luciferase assays. *C*, cells were co-transfected with p2.1, pTK-RL, and the indicated amount of expression vectors encoding either no protein (*EV*) or a dominant negative form of HIF-1α (*DN*). The total amount of expression vectors was adjusted to 500 ng with empty vector. The ratio of firefly to *Renilla* luciferase activity (*RLA*) was determined and normalized to the value obtained from nonhypoxic cells transfected with empty vector to obtain the relative luciferase activity. Results shown represent mean ± S.D. of three independent transfections.

(Roche Applied Science) (32). Samples were centrifuged at 10,000 × *g* to pellet cell debris. For HIF-1α and HIF-1β, 100-μg aliquots were fractionated by 7.5% SDS-PAGE and subjected to an immunoblot assay using mouse monoclonal antibody against HIF-1α (BD Biosciences, San Jose, CA) or HIF-1β (H1β234; Novus Biologicals, Littleton, CO) at 1:1000 dilution. Signal was developed using ECL reagent (Amersham Biosciences). For phosphorylated protein, HEK293 cells or HCT116 cells were serum-starved (0.1% fetal bovine serum for 24 h) and treated with NOC18, and 50-μg aliquots were analyzed using specific antibodies (1:1000 dilution) (Cell Signaling Technology, Beverly, MA). Signal was developed by using ECL reagents (Amersham Biosciences).

Inhibitor Treatments—PD98059, LY294002, genistein, or rapamycin was added 1 h before exposure to NOC18 or 1% O_2. CHX was added to the medium of HEK293 cells that were treated with NOC18, GSNO, or DFX for 4 h, and whole cell extracts were prepared at 15, 30, and 60 min.

RT-PCR—The protocol of RT-PCR is described elsewhere (33). Briefly, cells were lysed, and RNA was isolated with TRIzol reagent (Invitrogen). 0.5 μg of total RNA were subjected to first strand cDNA synthesis using the SuperScript II RT kit (Invitrogen) with random hexamers. cDNAs were amplified with TaqGold polymerase in a thermal cycler with the following primer pairs: HIF1A, GAAAGCGCAAGTCCTCAAA and CTATATGGTGATGATGTGGCACTA; VEGF, CCATGAACTTTCTGCTGTCTT and ATCGCATCAGGGGCACACAG; GLUT1, GGGCATGTGCTTCCAGTATGT and ACGAGGAGCACCGTGAAGAT; 18 S, ATCCTGCCAGTAGCATATGC and ACCCGGGTTGGTTTTGATCTG. For each primer pair, PCR was optimized for cycle number to obtain linearity between the amount of input RT product and output PCR product. Thermocycling conditions were 30 s at 94 °C, 60 s at 57 °C, and 30 s at 72 °C for 25 (HIF1A), 27 (VEGF), or 14 (18 S rRNA) cycles preceded by 10 min at 94 °C. PCR products were fractionated by 3% Nusieve agarose gel electrophoresis, stained with ethidium bromide, and visualized with UV.

Metabolic Labeling Assay—The protocol is described elsewhere (8). Briefly, a total of HEK293 cells were plated in a 10-cm dish, and 24 h later the cells were serum-starved for 20 h. The cells were pretreated with 500 μM NOC18 or 100 μM DFX for 30 min in methionine-free Dulbecco's modified Eagle's medium. [^{35}S]Met-Cys was added to a final concentration of 0.3 mCi/ml, and the cells were pulse-labeled for 20–40 min and then harvested. Whole cell extracts were prepared, and 1 mg of extract was precleared with 60 μl of protein A-Sepharose for 1 h. 20 μl of anti-HIF-1 antibody H1 67 was added to the supernatant and rotated overnight at 4 °C. 40 μl of protein A-Sepharose was added, rotated for 2 h at 4 °C, pelleted, and washed five times with 1 ml of radioimmune precipitation buffer. The samples were analyzed by SDS-polyacrylamide gel electrophoresis. The gel was dried and exposed to x-ray film.

Immunoprecipitation Assay—Cells were harvested in 200 μl of lysis buffer (Dulbecco's PBS (pH 7.4), 0.1% Tween 20, 1 mM sodium orthovanadate, and Complete protease inhibitor) and drawn through a 20-gauge needle four times. The lysate was incubated on ice for 1 h, followed by centrifugation at 14,000 rpm for 15 min. The cleared lysates were brought to a volume of 1 ml with lysis buffer followed by a 2-h incubation with 20 μl of anti-HA (Roche Applied Science) or anti-FLAG (Sigma) affinity matrix beads at 4 °C on a rotator. The beads were then

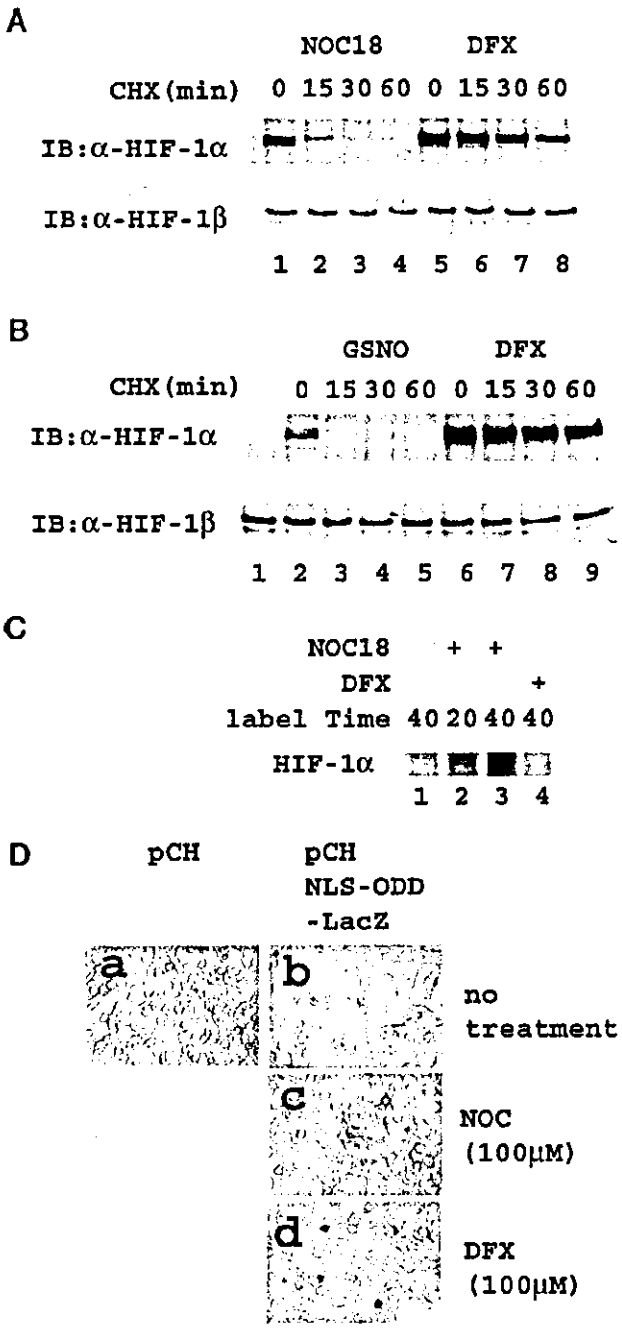

FIG. 4. **Effect of NOC18 and GSNO on HIF-1 protein stability and synthesis.** HEK293 cells were exposed to 500 μM NOC18 (*A*), 250 μM GSNO (*B*), or 100 μM DFX (*A* and *B*) for 4 h, and then CHX was added to a final concentration of 100 μM. The cells were incubated for 0–60 min, and whole cell lysates were subject to immunoblot (*IB*) assay using anti-HIF-1α (*top*) and HIF-1β (*bottom*) antibodies. *C*, pulse labeling of HEK293 cells. Serum-starved cells were pretreated with no drug, NOC18, or DFX for 30 min in Met-free medium. [^{35}S]Met-Cys was added, and the cells were incubated for 20 or 40 min prior to preparation of cell lysates and immunoprecipitation of HIF-1α. *D*, HEK293 cells were transfected with plasmid pCH-NLS-HIF-1α(574–603)-LacZ (*b–d*) or empty vector (*a*) and treated with NOC18 (*c*) or DFX (*d*). The cells were stained with X-gal to detect nuclear expression of β-galactosidase.

washed three times with lysis buffer. Protein was eluted by the addition of Laemmli sample buffer and analyzed by SDS-PAGE and immunoblot analysis (16).

In Vitro HIF-1α-VHL Interaction Assay—Glutathione *S*-transferase (GST)-HIF-1α(429–608) fusion protein was expressed in *E. coli* as described (16, 33). Biotinylated methionine-labeled proteins were generated in reticulocyte lysates using the TNT T7 coupled transcription/translation system using Transcend biotinylated tRNA (Promega). 25-μg aliquots of HEK293 cell lysate were preincubated with NO donor or DFX for 30 min at 30 °C, 2.5 μg of GST-HIF-1α(429–608) was added, and the mixture was incubated for 30 min at 30 °C. A 5-μl aliquot of *in vitro* translated biotinylated VHL protein was mixed with 4 μg of GST fusion protein in a final volume of 200 μl of binding buffer (Dulbecco's PBS (pH 7.4), 0.1% Tween 20) and incubated for 2 h at 4 °C with rotation followed by the addition of 10 μl of glutathione-Sepharose 4B beads (Amersham Biosciences) and incubation at 4 °C for 1 h. The beads were pelleted, washed 3 times in binding buffer, pelleted again, resuspended in Laemmli sample buffer, and analyzed by SDS-PAGE. Proteins were transferred to polyvinylidene difluoride membrane and visualized using streptavidin-labeled horseradish peroxidase and ECL reagent (Amersham Biosciences).

In Vitro Ubiquitination Assay—HEK293 cells were washed twice with cold hypotonic extraction buffer (20 mM Tris (pH 7.5), 5 mM KCl, 1.5 mM $MgCl_2$, 1 mM dithiothreitol) and lysed in a Dounce homogenizer. The cell extract was centrifuged at 10,000 × *g* for 10 min at 4 °C, and the supernatant was stored at 70 °C. Ubiquitination assays were performed as described previously (33). 2 μl of HA-HIF-1α that was *in vitro* translated (TNT Quick Coupled Transcription/Translation System; Promega) in the presence of [^{35}S]methionine was incubated at 30 °C in a volume of 40 μl containing 27 μl (50 μg) of cell extract, 4 μl of 10× ATP-regenerating system (20 mM Tris (pH 7.5), 10 mM ATP, 10 mM magnesium acetate, 300 mM creatine phosphate, 0.5 mg/ml creatine phosphokinase), 4 μl of 5 mg/ml ubiquitin (Sigma), 1 μl of 150 μM ubiquitin aldehyde (Sigma), and HA-HIF-1α was recovered using anti-HA-agarose beads, which were then mixed with SDS sample buffer and boiled for 5 min. The eluates were analyzed by SDS-PAGE and autoradiography.

Reporter Gene Assays—Reporter assays were performed in Hep3B cells and HEK293 cells (32, 34). 5 × 10^4 cells were plated per well on the day before transfection. In each transfection, the indicated dose of test plasmids, 200 ng of reporter gene plasmid, and 50 ng of the control plasmid pTK-RL (Promega), containing a thymidine kinase promoter upstream of *Renilla reniformis* (sea pansy) luciferase coding sequences, were premixed with Fugene 6 transfection reagent (Roche Applied Science). In each assay, the total amount of DNA was held constant by the addition of empty vector. After treatment, the cells were harvested, and the luciferase activity was determined using the Dual-Luciferase Reporter Assay System (Promega). The ratio of firefly to sea pansy luciferase activity was determined. For each experiment, at least two independent transfections were performed in triplicate.

X-gal Staining—HEK293 cells were washed twice with PBS, fixed with 1% formaldehyde, 0.2% glutaraldehyde solution, washed twice with PBS, and then treated with an X-gal staining solution (5 mM potassium ferrocyanide, 5 mM potassium ferricyanide, 1 mM $MgCl_2$, and 0.04% X-gal) at 37 °C (28).

RESULTS

NO Donors Activate HIF-1 under Nonhypoxic Conditions—To study the effect of NO on HIF-1 activation, we tested several NO donors. NORs and NOCs spontaneously release NO with different kinetics (see "Experimental Procedures"), whereas GSNO and SNP require cellular thiol for NO release. HEK293 cells were exposed to the compounds for 1–4 h at 20% O_2, harvested, and subjected to immunoblot analysis using anti-HIF-1α or anti-HIF-1β antibody (Fig. 1*A*). Neither NOR4 nor NOR5 induced HIF-1α protein accumulation (*lanes 2–5*). In contrast, exposure of cells to NOC18 or GSNO efficiently induced HIF-1α protein accumulation comparably with 100 μM DFX (*lanes 6–8*, *12*, and *13*). SNP did not induce HIF-1α accumulation (*lanes 10* and *11*). Expression of HIF-1β was not affected by NO donors or DFX. NOCs induced accumulation of HIF-1α with quite different kinetics as compared with GSNO. NOC18-induced accumulation was detected as early as 30 min and lasted no less than 8 h. The effect of GSNO peaked at 1 h (*lane 8*) and was lost by 4 h after the addition (*lane 9*).

NOC18 induced HIF-1α accumulation in a dose-dependent manner up to 500 μM (Fig. 1*B*). Induction by GSNO was saturated at a concentration of 100 μM. The accumulation of HIF-1α induced by NOC12, which releases NO by the same mechanism

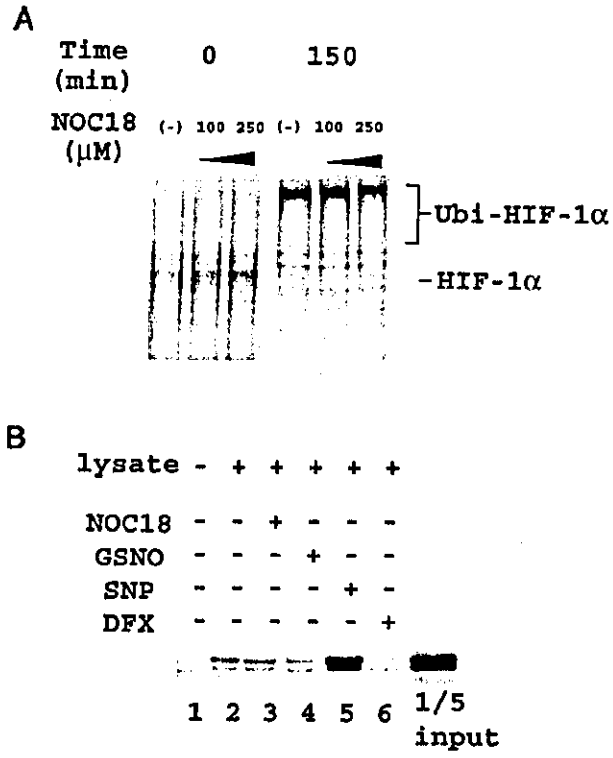

FIG. 5. **Analysis of HIF-1α ubiquitination and interaction with VHL.** *A*, *in vitro* ubiquitination assay. Lysates prepared from cells exposed to vehicle (−) or NOC18 (+) for 4 h were incubated with *in vitro* translated HIF-1α in the presence of ubiquitin and ATP for 0 or 150 min. Polyubiquitinated forms of HIF-1α (Ubi-HIF-1α) were identified by their reduced mobility after PAGE. *B*, GST-HIF-1α(429–608) fusion protein was incubated with *in vitro* translated VHL in the presence of PBS or lysates untreated or treated with the indicated reagents. Glutathione-Sepharose beads were used to capture GST-HIF-1α, and the presence of associated VHL in the samples was determined by PAGE. One-fifth of the input VHL protein was also analyzed. *C* and *D*, FLAG-tagged HIF-1α and HA-tagged VHL were expressed in HEK293 cells. Cells were treated or untreated with 250–500 μM NOC18 or 100 μM DFX for 2 h and harvested. Lysates were incubated with anti-FLAG affinity beads, and captured protein was eluted and analyzed by SDS-PAGE. Epitopes were detected with anti-FLAG (*top*) or anti-HA (*bottom*) antibody. *IP*, immunoprecipitation; *IB*, immunoblot.

as NOC18 but has a different NO-releasing time constant, was stronger than that induced by NOC18 at 30 min at a concentration of 250 μM (Fig. 1*C*, *top panel*). However, the induction of HIF-1α was dose-dependent such that the effect of 40 μM NOC12 was weaker than 500 μM NOC18 (Fig. 1*C*, *bottom panel*).

We screened other cell lines for the effect of NO donors on HIF-1α protein levels. 500 μM NOC18 induced HIF-1α accumulation in Hep3B human hepatocellular carcinoma cells and HCT116 human colorectal carcinoma cells as strongly as 100 μM DFX (data not shown). NOC18 also induced HIF-1α in human umbilical vein endothelial cells (data not shown). These results indicate that the effect of NOC18 on HIF-1α expression is observed in multiple transformed and primary cell types.

We investigated by RT-PCR whether NO donors induced gene expression downstream of HIF-1. VEGF and GLUT1 mRNA expression was induced by NOC18 treatment under nonhypoxic conditions (Fig. 2). In contrast, HIF-1α mRNA expression was not affected by NOC18 treatment, indicating that the effect of NOC18 occurs at the level of HIF-1α protein expression. HEK293 cells were transfected with the reporter p2.1, containing a HIF-1-dependent HRE, or p2.4, containing a mutated HRE. NOC18 induced HRE-dependent gene expression in a dose-dependent manner comparably with DFX or 1% O_2 (Fig. 3, *A* and *B*). The mutated reporter p2.4 was not activated by NOC18 (Fig. 3*B*), and expression of a dominant negative form of HIF-1α reduced p2.1 reporter gene expression (Fig. 3*C*), providing evidence that the gene activation was HRE- and HIF-1-dependent. NOC18 also induced dose-dependent transcription of a reporter gene containing the VEGF promoter encompassing nucleotides −2274 to +379 relative to the transcription start site (Fig. 3*D*).

NOC18 Does Not Prolong HIF-1α Protein Half-life—To determine whether NOC18 treatment affected HIF-1α protein half-life, HEK293 cells were treated with NOC18 or DFX for 4 h to induce HIF-1α expression, and then CHX was added to block ongoing protein synthesis. In the presence of CHX, the half-life of HIF-1α was >30 min in DFX-treated cells but <15 min in NOC18-treated cells (Fig. 4*A*). Similarly, the half-life of GSNO-induced HIF-1α is <15 min in the presence of CHX (Fig. 4*B*). These results indicate that HIF-1α expression in NOC18-treated cells is dependent upon ongoing protein synthesis. Similar results were observed in Hep3B cells and human umbilical vein endothelial cells (data not shown).

To analyze the rate of HIF-1α synthesis, serum-starved HEK293 cells were pretreated with NOC18 or DFX for 30 min and then pulse-labeled with [^{35}S]Met-Cys for 20 or 40 min, followed by immunoprecipitation of HIF-1α (Fig. 4*C*). In contrast to control serum-starved cells (Fig. 4*C*, *lane 1*), ^{35}S-labeled HIF-1α was clearly increased in NOC18-treated cells (*lanes 2* and *3*), whereas the amount of labeled HIF-1α protein was not increased in cells treated with DFX (*lanes 4*). Thus, both the cycloheximide addition and metabolic labeling experiments provide evidence for increased synthesis of HIF-1α in response to NOC18 treatment.

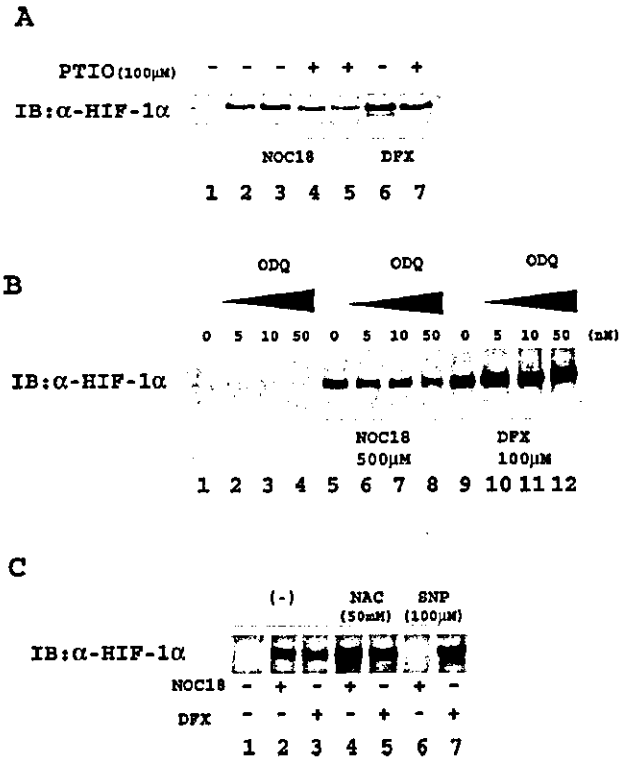

FIG. 6. **Effect of NO scavenger, guanylate cyclase inhibitor, and antioxidant on HIF-1α induction by NOC18.** HEK293 cells were treated with 250 μM NOC18 or 100 μM DFX with or without carboxyl-PTIO (*A*), ODQ (*B*), or *N*-acetyl cysteine (*NAC*) (*C*) for 4 h and harvested. Then the lysates were subjected to immunoblot (*IB*) assay with anti-HIF-1α antibody.

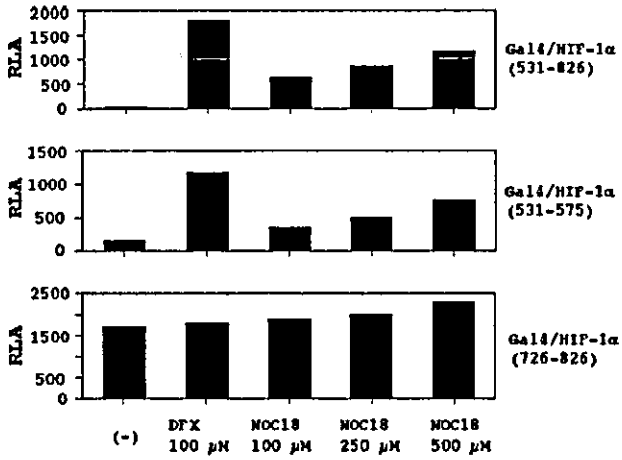

FIG. 7. **Effects of NOC18 on HIF-1α transactivation domain function.** Constructs encoding the GAL4 DNA-binding domain (amino acids 1–147) fused to the indicated amino acids of HIF-1α were analyzed for their ability to transactivate reporter gene GAL4E1bLuc, containing five GAL4-binding sites. HEK293 cells were co-transfected with pTK-RL (50 ng), GAL4E1bLuc (100 ng), and GAL4-HIF-1α fusion protein expression plasmids (100 ng). Cells were treated with 100 μM DFX or 100–500 μM NOC18 for 16 h and then harvested. The ratio of firefly to *Renilla* luciferase activity was determined and normalized to the value obtained from untreated cells transfected with plasmid encoding GAL4(1–147) to obtain the relative luciferase activity (*RLA*).

We also assayed the stability of a fusion protein, consisting of a nuclear localization signal (NLS), β-galactosidase sequences (encoded by the *lacZ* gene), and HIF-1α residues 548–603. The NLS-LacZ-HIF1α(548–603) expression vector was transfected into HEK293 cells, and β-galactosidase activity was analyzed by X-gal staining after incubation of the cells in the presence of 500 μM NOC18 or 100 μM DFX. There was essentially no X-gal staining in cells that were transfected with empty vector, transfected with NLS-LacZ-HIF1α(548–603) without treatment, or transfected with NLS-LacZ-HIF-1α(548–603) with NOC18 treatment (Fig. 4*D*). In contrast, significant X-gal staining was detected in NLS-LacZ-HIF-1α(548–603)-transfected cells that were treated with DFX, which inhibits O_2-dependent degradation mediated by the HIF-1α domain of the fusion protein.

NOC18 Does Not Affect the Interaction between HIF-1α and VHL in Vitro or in Vivo—Under hypoxic conditions, VHL-dependent ubiquitination of HIF-1α is inhibited (12–14). To determine whether NOC18 treatment affects ubiquitination, an *in vitro* assay was performed using lysates prepared from control and NOC18-treated cells. As shown in Fig. 5*A*, there was no significant difference detected between lysates from NOC18-treated or untreated cells with respect to their ability to ubiquitinate HIF-1α.

Incubation of a GST-HIF-1α(429–608) fusion protein with lysate from untreated cells resulted in prolyl hydroxylation of HIF-1α and interaction with VHL (Fig. 5*B*, *lane 2*). Lysate from cells treated with DFX did not promote interaction of GST-HIF-1α(429–608) with VHL (*lane 6*). In contrast, lysate from cells treated with NOC18 promoted the interaction (*lane 3*), similar to control lysates, again providing evidence that NOC18 treatment does not induce HIF-1α expression by inhibiting VHL-mediated ubiquitination. Similar results were obtained from experiments using rabbit reticulocyte lysates (which also have HIF-1α prolyl hydroxylase activity) instead of HEK293 cell lysates (data not shown). Remarkably, lysate from GSNO-treated cells partially inhibited the interaction of GST-HIF-1α(429–608) with VHL (*lane 4*), whereas lysate from SNP-treated cells dramatically increased the interaction (*lane 5*).

HEK293 cells were co-transfected with expression vectors encoding HA-tagged VHL and FLAG-tagged HIF-1α. Aliquots of whole cell lysates were analyzed for expression of the proteins directly or following immunoprecipitation of HA-VHL or FLAG-HIF-1α. HIF-1α was present in anti-HA immunoprecipitates from cells co-expressing HA-VHL and FLAG-HIF-1α (Fig. 5*C*, *lane 3*). Exposure of cells to NOC18 did not alter the interaction of HA-VHL and FLAG-HIF-1α (Fig. 5*C*, *lanes 4* and *5*), consistent with the inability of NOC18 to inhibit VHL and HIF-1α interaction *in vitro*. In contrast, DFX treatment inhibited the interaction (*lane 6*). FIH-1 is the asparagine hydroxylase that negatively regulates HIF-1α transactivation domain function under nonhypoxic conditions (16, 17). The interaction between HA-FIH-1 and FLAG-HIF-1α was not affected by either NOC18 or DFX (Fig. 5*D*). Taken together, results presented in Fig. 5 indicate that the molecular mechanism of NOC18 action is distinct from the inhibition of hydroxylase activity that occurs in cells exposed to hypoxia or DFX.

Impact of NO Scavenger, Guanyl Cyclase Inhibitor, and Antioxidant on NOC18-induced HIF-1α Accumulation—To examine signal transduction pathways mediating effects of NO donors on HIF-1α protein induction, the NO scavenger carboxyl-PTIO was utilized (35). Carboxyl-PTIO significantly suppressed HIF-1α accumulation induced by NOC18 but not by DFX (Fig. 6*A*). Carboxyl-PTIO by itself did not have any effects. Next we examined the impact of guanylyl cyclase activity on HIF-1α accumulation. NO stimulates the activity of guanylyl cyclase, which catalyzes the production of cGMP, an important second messenger for signal transduction. In HEK293 cells, the specific guanyl cyclase inhibitor ODQ did not affect NOC18-induced HIF-1α accumulation (Fig. 6*B*), providing evidence that the guanylyl cyclase-cGMP pathway does not contribute to

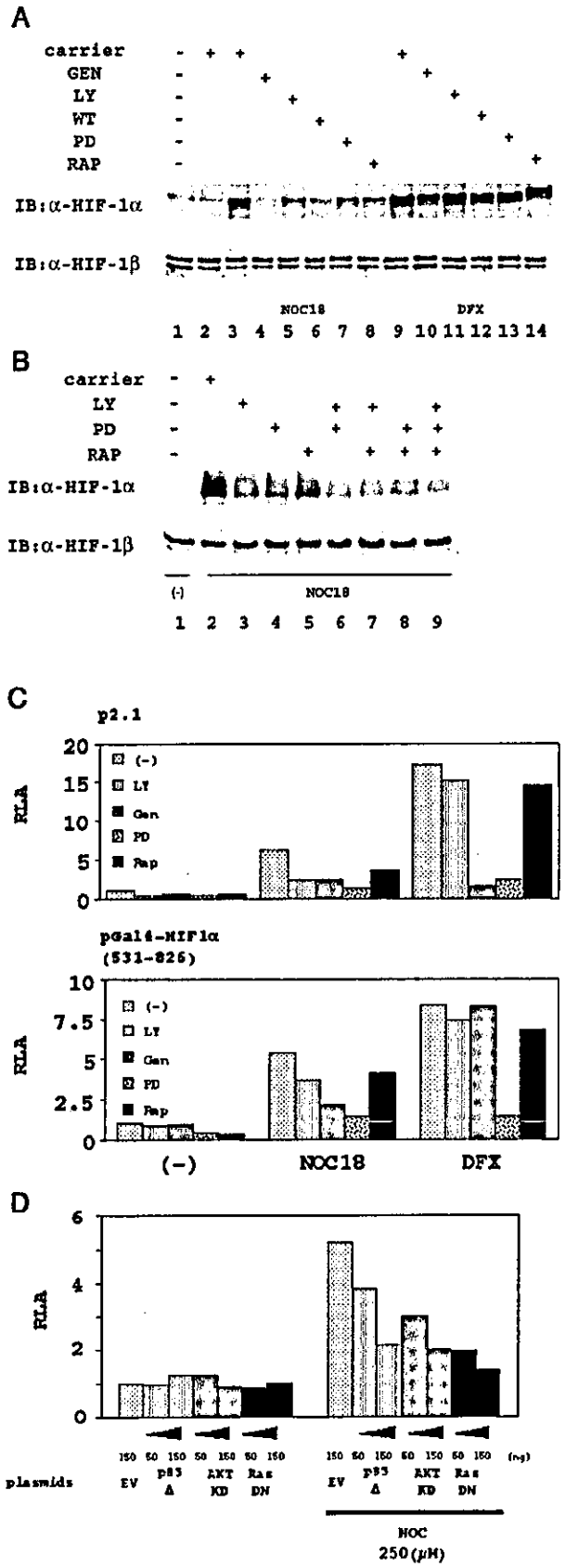

FIG. 8. **Effect of kinase inhibitors on the induction of HIF-1α protein and transactivation.** *A* and *B*, HEK293 cells were exposed to vehicle, 500 μM NOC18, or DFX in the presence (+) of 100 μM genistein (*GEN*), 5 μM LY294002 (*LY*), 50 μM PD98059 (*PD*), 100 nM wortmannin (*WT*), or 200 nM rapamycin (*Rap*) and harvested after 4 h for analysis of HIF-1α protein. HRE-dependent gene expression (*C* (*top*) and *D*) or HIF-1α transactivation domain function (*C*, *bottom*) were analyzed using p2.1 or Gal4-HIF-1α(531–826) and GAL4E1bLuc, respectively. Cells were pretreated with LY294002, genistein, PD98059, or rapamycin and exposed to 250 μM NOC18 or 100 μM DFX. *D*, cells were transfected with an expression vector encoding a dominant negative form of p85 PI3K, Akt, or Ras. *IB*, immunoblot.

HIF-1α accumulation induced by NOC18.

NO is a radical, and equimolar amounts of O_2^- and NO form peroxynitrite ($ONOO^-$), which decomposes at physiological pH to generate oxidant with similar reactivity to the hydroxyl radical. To examine whether the intracellular redox state modulates NOC18-induced HIF-1α accumulation, HEK293 cells were treated with NOC18 in the presence of 50 mM *N*-acetyl cysteine (*NAC*) (Fig. 6*C*). *N*-acetyl cysteine treatment did not affect HIF-1α levels, suggesting that thiol-mediated redox status does not play a critical role in NOC18-induced HIF-1α expression. Transient overexpression of the intracellular redox regulator thioredoxin also did not affect induction of HIF-1α expression by NOC18 (data not shown).

HIF-1α-mediated Transactivation in Response to NOC18 Treatment—We next investigated the impact of NOC18 on HIF-1α transcriptional activity. There are two independent transactivation domains (TADs) present in HIF-1α, which are designated as the amino-terminal (amino acids 531–575) and carboxyl-terminal (amino acids 786–826) TADs (TAD-N and TAD-C, respectively) (24). Steady-state levels of proteins consisting of the GAL4 DNA-binding domain fused to HIF-1α TADs (GAL4-HIF-1α(531–575), GAL4-HIF-1α(531–826), and GAL4-HIF-1α(786–826)) are similar under hypoxic and nonhypoxic conditions (24). These GAL4-HIF-1α fusion constructs can thus be used to examine the transcriptional activity of HIF-1α independent of its protein expression (24, 32). Transactivation mediated by GAL4-HIF-1α(531–826), which contains both TAD-N and TAD-C, or GAL4-HIF-1α(531–575), which contains only TAD-N, is increased in cells exposed to hypoxia or DFX (24). In contrast, GAL4-HIF-1α(786–826), which contains only TAD-C, is constitutively active in untreated cells. NOC18 treatment increased transactivation mediated by GAL4-HIF-1α(531–826) or GAL4-HIF-1α(531–575) in a dose-dependent manner, whereas transactivation mediated by GAL4-HIF-1α(786–826) was not increased by exposure of cells to NOC18 or DFX (Fig. 7). These results demonstrate that NOC18 not only promotes accumulation of HIF-1α but also enhances HIF-1α transcriptional activity.

Effect of Kinase Inhibitors on NOC18-induced HIF-1 Activation—HEK293 cells were pretreated with LY294002, genistein, PD98059, or rapamycin, which are selective pharmacologic inhibitors of PI3K, tyrosine kinases, MEK, and FRAP/mTOR kinase activity, respectively. All of the agents inhibited the induction of HIF-1α protein expression in NOC18-treated cells (Fig. 8*A*). The combination of LY294002, PD98059, and rapamycin markedly inhibited NOC18-induced HIF-1α expression (Fig. 8*B*). In contrast to their effects on HIF-1α protein expression induced by NOC18 treatment, LY294002 or PD98059 had little inhibitory effect on the expression of HIF-1α in DFX-treated HEK293 cells (Fig. 8*A*, *lanes 9–14*).

LY294002 and rapamycin inhibited expression of the HIF-1-dependent reporter gene p2.1 induced by NOC18 but not by DFX, whereas genistein and PD98059 inhibited both NOC18- and DFX-induced reporter gene expression (Fig. 8*C*, *top*). Interestingly, the stimulation of HIF-1α transactivation domain function by NOC18 was also blocked by kinase inhibitors, whereas only genistein blocked DFX-induced transactivation

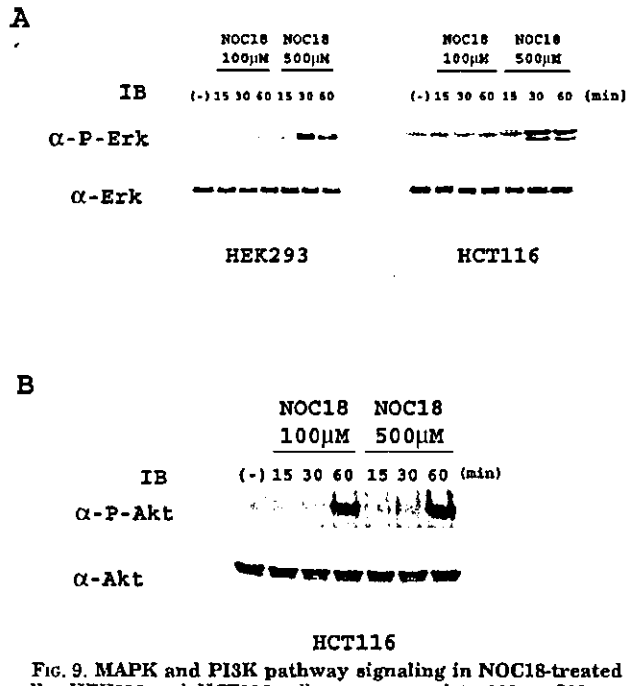

FIG. 9. **MAPK and PI3K pathway signaling in NOC18-treated cells.** HEK293 and HCT116 cells were exposed to 100 or 500 μM NOC18. Whole cell lysates were prepared after 15, 30, or 60 min and subjected to immunoblot (*IB*) assays using antibodies specific for phosphorylated (Thr-202/Tyr-204) or total $p42^{ERK2}/p44^{ERK1}$ MAPK (*A*) and phosphorylated (Ser-473) or total AKT (*B*).

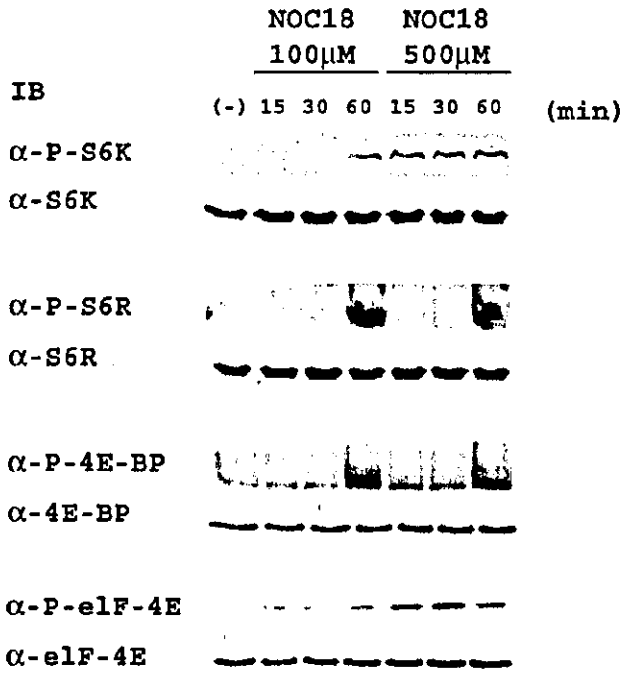

FIG. 10. **Phosphorylation of the translational regulators $p70^{S6K}$, S6 ribosomal protein, and eIF-4E in NOC18-treated HCT116 cells.** Cells were serum-starved for 24 h prior to NOC18 treatment. Whole cell extracts were prepared after NOC18 stimulation and subjected to immunoblot (*IB*) assays using antibodies specific for phosphorylated (Thr-421/Ser-424) or total $p70^{S6K}$, phosphorylated (Ser-235/236) or total S6 ribosomal protein (*S6R*), phosphorylated (Ser-65) or total 4E-BP, and phosphorylated (Ser-209) or total eIF-4E.

(Fig. 8*C*, *bottom*). These results provide further evidence that NOC18 and DFX induce HIF-1 by distinct molecular mechanisms. Moreover, NOC18-induced HRE-dependent gene expression was suppressed by a dominant negative form of PI3K p85 subunit, AKT, or Ras, indicating critical roles of these signaling proteins in transducing the effects of NOC18 to HIF-1 (Fig. 8*D*).

NOC18-induced Activation of MAPK, PI3K, and Translational Regulators—HIF-1 activity induced by the stimulation of receptor tyrosine kinases or G protein-coupled receptors requires MAPK and PI3K signaling (10, 36). To determine whether the MAPK and PI3K pathways were activated in NOC-18-treated cells, the phosphorylation of $p42^{ERK2}/p44^{ERK1}$ and AKT were analyzed in HEK293 cells and HCT116 cells. Increased phosphorylation of $p42^{ERK2}/p44^{ERK1}$ (Fig. 9*A*) and AKT (Fig. 9*B*) was induced by NOC18 treatment in both cell types.

The signal transduction pathway involving PI3K, AKT, and mTOR has been shown to regulate protein translation via phosphorylation of $p70^{S6K}$, the S6 ribosomal protein, and 4E-BP1. In both HCT116 cells (Fig. 10) and HEK293 cells (data not shown), the phosphorylation of $p70^{S6K}$, S6, and 4E-BP1 was induced by NOC18 stimulation in a dose- and time-dependent manner. The mRNA cap-binding protein eIF-4E was also phosphorylated by NOC18 treatment of HCT116 cells (Fig. 10). This result is consistent with studies indicating that ERK activates the MAPK signal-integrating kinases, MNK1 and MNK2, which in turn phosphorylate eIF-4E (37, 38).

DISCUSSION

The studies reported above demonstrate that treatment of several different cell types with the NO donor NOC18 induces HIF-1α protein expression and HIF-1 transcriptional activation, resulting in VEGF and GLUT1 mRNA expression. NOC18 treatment did not increase the half-life of HIF-1α protein, did not inhibit the interaction between HIF-1α and VHL, and did not inhibit the ubiquitination of HIF-1α, indicating that the mechanism of NOC18 action does not involve inhibition of HIF-1α prolyl hydroxylation. Rather than increasing the stability of HIF-1α, the data suggest that NOC18 increases the rate of HIF-1α protein synthesis.

Whereas exposure of cells to hypoxia or DFX decreases HIF-1α protein degradation, exposure of cells to heregulin, IGF-1, insulin, or prostaglandin E_2 increases HIF-1α protein synthesis (8–10, 36). In previous studies of MCF-7 and HCT116 cells, the effect on protein synthesis was documented by cycloheximide inhibition and by pulse-chase experiments (8). In the present study, we also confirmed that NOC18 treatment stimulated the synthesis of HIF-1α but had no effect on HIF-1α protein stability in HEK293 cells. Thus, as in the case of growth factor-treated cells, the increased expression of HIF-1α protein in NOC18-treated cells is due to increased synthesis.

As previously observed in growth factor-treated cells, the effect of NOC18 is dependent upon its activation of the PI3K and MAPK pathways. Dependence on MEK activity for phosphorylation of 4E-BP1 and $p70^{S6K}$ has been demonstrated in other cellular contexts. In the case of IGF-1-stimulated colon cancer cells, both MEK and PI3K are required for activation of $p70^{S6K}$, with MEK inhibitors preventing the phosphorylation of Thr-421/Ser-424 in the Thr-389 by mTOR (39). ERK has been shown to phosphorylate 4E-BP1 *in vitro* (40). The MEK-ERK pathway also stimulates the phosphorylation of eIF-4E, which is required for its mRNA cap binding activity (37). Thus, NOC signaling both derepresses (via phosphorylation of 4E-BP1) and activates (via phosphorylation of eIF-4E and $p70^{S6K}$) protein synthesis. The effects of NO donors may not be specific for HIF-1α. The known targets for phosphorylation by mTOR are regulators of protein synthesis. The translation of several